Intervertebral movement analysis of the cervical spine:

Prediction and categorising of cervical joint motion

10^{th} Semester of the Master in Biomedical Engineering and Informatics, Master Thesis

Project group: 17gr9413
Burcu Betina Yüksel

AALBORG UNIVERSITY
DENMARK

Aalborg University
School of Medicine and Health
Fredrik Bajers Vej 7
DK-9220 Aalborg Øst

School of Medicine and Health
Fredrik Bajers Vej 7
DK-9220 Aalborg Ø
http://smh.aau.dk

AALBORG UNIVERSITY
STUDENT REPORT

Title:
Intervertebral movement analysis of the cervical spine: Prediction and categorising of cervical joint motion

Theme:
Master's thesis

Project Period:
4. semester master Autumn 2017

Project Group:
17gr9413

Participants:
Burcu Betina Yüksel

Supervisors:
Lasse Riis Østergaard
Maciej Plocharski
René Lindstrøm

Copies: Online

Page Numbers: 45

Date of Completion:
January 5^{th} 2018

Abstract:

Complications related to damaged cervical spine movement, can cause chronic conditions such as whiplash, migraine, constant pain in the head and neck, tinnitus etc. Neck pain has a prevalence of 570,000 for men and women in Denmark, with an annual treatment costs of 920 million DKK. Range of motion (ROM) is the range of physiologic intervertebral motion mesured from the neutral position to measure cervical flexion and extension. The flexion and extension motion of the cervical spine has been assumed to be linear and continuous until recently. Data consisting of 33 participants in flexion, and 32 participants in extension was provided by Aalborg University. In this study, a predictive analysis of a healthy cervical spine movement in flexion and extension direction has been developed. By developing a prediction analysis using the regression model Multiple Linear Regression, all movements of the cervical joint were predicted. This was done by training and testing on all cervical joints. To demonstrate if specific characteristic joints could describe joint motions in the upper part of the cervical spine "C0/C1", "C3/C4" and "C4/C5" were used to estimate the regression.
The predicted data set was compared to manually calculated rotations done by a clinician and resulted in a R^2 (R-squared) value of 0.95 across the cervical joints.

Resumé

Komplikationer i forbindelse med beskadiget nakkesøjle, kan medføre forskellige kroniske lidelser som piskesmæld, migræne, vedvarende smerte i hovedet og nakke, tinnitus mm. Den Nationale Sundhedsprofil har i 2010 lavet en opgørelse, hvoraf 200.000 mænd og 370.000 kvinder har vist at have nakkesmerter i Danmark. Med en årlig omkostning på 920 millioner kroner i behandling og 2.030 millioner kroner i tabt arbejdsproduktion, er nakkesmerter et udbredt fænomen for økonomiske omkostninger for samfundet [4].

For at åbne op for diagnosticeringsmuligheder af nakkesmerter, kan målinger af den intervertebrale kinematik bruges til at evaluere bevægelsen i nakken ved en funktionel undersøgelse. Range of motion (ROM) er området af den fysiologiske bevægelse fra neutral position til enten fleksion eller ekstension retning. I dette studie bruges ROM i forbindelse med nakkeledets bevægelse.

Manuel segmentering og sporing af nakkehvirvler og dens områder i videosekvenser er en besværlig og tidskrævende proces. Semi-automatiske metoder er blevet udviklet, hvor templateprocessen kræver detaljeret markering af hver hvirvel i den første sekvens. Desuden kan det være udfordrende at spore nakkehvirvlen gennem hele videosekvensen ved øvre og nedre hvirvler, enten grundet lokalisering af hvirvlen, eller ændring af form under fleksion eller ekstensionsbevægelse. Baseret på nuværende viden, er følgende to formål identificeret:

Formål 1 Prædiktering af den totale fleksion- og ekstensionsbevægelse af hvert nakkeled, og undersøge om hvorvidt der er nogle led der er mere karakteristiske til at prædiktere bevægelsen af den øverste nakkehvirvel "C0/C1".

Formål 2 Undersøge hele fleksion- og ekstensionsbevægelsen med hensyn til anti-retnings ledbevægelser, og dermed opdele forsøgspersoner i undergrupper af lignende bevægelsesmønstre.

Prædiktioner af nakkehvirvler blev udført ved anvendelse af multiple lineær regressionsanalyse. Kategorisering af forsøgspersoner blev dannet ved klyngedannelsesmetoden k-means.

Resultatet viste at den totale fleksion- og ekstensionsbevægelse i det øverste nakkeled "C0/C1", kan med variationer prædikteres ved anvendelse af alle seks led som prædiktorer. Samtidig kan det øverste nakkeled "C0/C1" også prædikteres ved kun at bruge to led som prædiktorer. Under gruppering af forsøgspersoners bevægelsesmønstre, var opdelingen af prædikteret data og studie data ikke fuldstændig identisk. Den forskellige opdeling kan skyldes de varierende anti-retningsbevægelser hos enkelte forsøgspersoner. Grupperingen kan således bruges til at åbne op for behandlingsmulighder afhængigt af undergruppens oplsyninger.

Preface

This 10^{th} semester master thesis has been written by Burcu Betina Yüksel (group 17gr9413) during the 4^{th} semester of the Master programme in Biomedical Engineering and Informatics at Aalborg University. The master thesis title is "Intervertebral movement analysis of the cervical spine: prediction and categorising of cervical joint motion".
The thesis has been supervised by Associate Professor Lasse Riis Østergaard, Ph.D, Research Assistant Maciej Plocharski, Ph.D and Post.doc. Rene Lindstrøm, Ph.D.

Aalborg University, 5^{th} of January 2018

Reading Guide

Applied literature is presented in chronological order in the bibliography in the back of the report. Sources are referenced using the Vancouver method, with the references consisting of a number that increases with each new source, an example: [1], [2] etc. Web pages are specified by, information about the author(s), title, URL address, and access data.
All references are set after a period, whether it is after a single sentence or a smaller section, the reference has been used for everything up to the previous reference. Figures and tables are numbered by chapter and section, where figures without any references in the caption are self made.

In chapter 1 and 2, the thesis' overall dilemma and problem analysis are presented.
Chapter 3 contains aim and solution strategy for the study.
Chapter 4 contains materials and methods, where this chapter is divided into three parts:
1) Prediction using six cervical joints
2) Prediction using two cervical joints
3) Division into subgroups of motion pattern
The results are found in chapter 5 and chapter 6 and 7 contain a discussion and conclusion, respectively.

Contents

1 | Introduction

Cervical spine injury can occur through hyperextension when the head accelerates forward and then rotate backwards. In case of sudden change of position, for example in a fall or under fast acceleration or deceleration, the muscles that ensure balance will fail to stabilize the head. This can displace the cervical vertebra and can result in damage to both muscles and ligaments, thereby cause damage to the spinal cord [1]. Exaggerated motion can be indicative of physical spinal damage and too limited motion can cause stiffness and pain [2].

Complications with damaged cervical spine motion can cause most common chronic problems as: whiplash, continuous head and neck pain, migraine, reduced activity, tinnitus etc. Whiplash refers to the mechanism or movement, when the body is affected by a sudden violent force, typically in vehicular accidents. The symptoms may further cause reduced quality of life and impaired living conditions [3, 2]. In Denmark, neck pain has prevalence of 570,000 for men and women, where employees with neck pain have 16% more sick days compared to healthy employees. The annual treatment costs are 920 mio. kr. and it has been reported that every year, neck pain costs 2.3 mio. kr. due to lost productivity [4].

In order to assess the cervical spine function in healthy subjects and those with a cervical spine injury, Range of motion (ROM) is used to measure cervical flexion and extension. ROM is the range of physiologic intervertebral motion measured from the neutral position [5]. Reduced cervical movements are referred to as deficient movements and can be helpful in diagnosis in clinical context.

The flexion and extension motion of the cervical spine has been assumed to be linear and continuous. This assumption has been the reason why the cervical spine is modelled as a spring-like spine structure with linear and continuous motion patterns with linear joint muscles [5].
Despite the established knowledge about the cervical spine motion, recent studies do not support the linear and continuous spring-structure of joint motion during flexion and extension in healthy subjects [5, 6].

Intervertebral joint motion is a research field, and recent studies have investigated the cervical vertebra motion using video fluoroscopy [7, 5]. Video fluoroscopy is a functional examination technique and enables dynamic real-time scans during motion [8].

In a new observational study, the physiology of the cervical spine motion has recently been examined by [Wang et al., 2017]. Video fluoroscopy was used for visual real-time tracking of intervertebral movements. Vertebral motions opposite the intended directional motion have been discovered in healthy subjects. These opposite motions are defined as anti-directional joint motion of the pro-directional joint motion. Anti-directional joint motion represented approximately 40% of the pro-directional joint motion. While the upper cervical joints (C0-C2) bended backwards, it was found that the lower cervical joints (C6-C7) were flexing, and the other way around. [5]

This new observation about anti-directional motion in the cervical spine motion, leads to further research of the cervical spine motion. As opposed to the spring-like structure, the new knowledge can be used to quantify the anti-directional joint movement. This can be used to classify joint movements in healthy as well as in patients with injuries in the cervical spine, to obtain the actual cervical spine motion to offer the best treatment option for patients with neck pain.

The movement of the cervical spine has been examined with image analysis methods. This study has been aimed at using the statistical approach, multiple linear regression (MLR) analysis, to prediction and categorisation of the entire joint articulation. MLR is carried out to predict the values of a dependent variable Y, given a set of independent variables (X_1, X_2,...,X_k). The anti-directional joint motion during neck flexion and extension of healthy participants was taken into consideration in this approach. In this context, it is known that the individual joints in the neck behave differently from each other, and have different characteristics. It was examined whether a certain cervical joint, had more significance for detecting the upper cervical joint movement.

Predicting and categorising neck flexion and extension into groups of similar joint motion patterns, gives a deeper understanding of intervertebral movement. This might improve the understanding of cervical spine disorders, and opens new possibilities for new treatments. Clinicians will potentially be able to remedy patients with a painful neck injury, depending on which joint group their intervertebral movement belongs to.

On this basis, the solution strategy was divided into three parts. In the first part, all cervical vertebrae were used to train and test, in order to predict the entire joint motion. In the second part, only two joints were used train and test to predict a single joints' motion. The aim of the last part was categorise the neck flexion and extension into groups of similar joint motion patterns.

2 | Problem Analysis

In order to analyse, understand and improve malfunctions of the cervical spine, it is important to have a knowledge of the anatomy and physiology of a normal functioning human cervical vertebra.

2.1 Cervical Vertebrae

Human spine consist of 33 vertebrae, where the vertebrae are divided into regions: cervical, thoracic, lumbar, sacrum, and coccyx. Spinal cord is the bodies main upright support, where the vertebrae in each region have different features, that help them perform their main functions [1].
Seven vertebrae are connected by the intervertebral disc, ligaments and other soft tissues, forming the cervical spine (C1-C7), where the top C1 connects to the bottom of the skull. Cervical spine has the important job of supporting the skull and allowing the head to move. Furthermore, it curves inwards and is taught to balance the head's weight on the cervical vertebrae. The cervical spine also protects the spinal cord, the connection between the brain and the rest of the body [1].

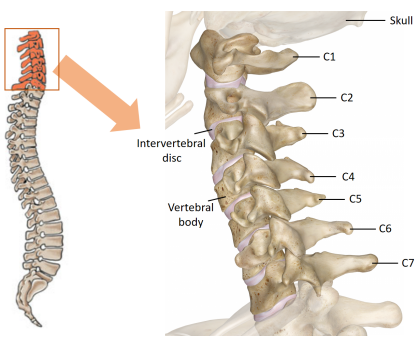

(a) Cervical vertebrae anterior view

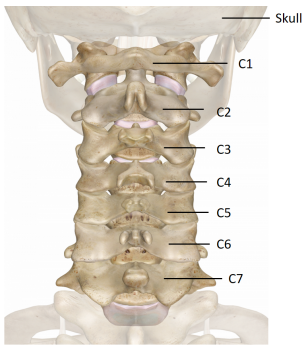

(b) Cervical vertebrae posterior view

Figure 2.1: (a) and (b) show a model of a normal cervical vertebra with anterior and posterior view.

C1 - Atlas

The C1 vertebra, known as the atlas, is the most superior vertebrae in the spinal column. It plays vital roles in the support of the skull, spinal cord, and vertebral arteries and provides attachment points for several muscles of the neck [1]. Compared to the other vertebrae in the spine, the vertebral foramen is larger in C1, allowing significant space for movement of the soft nervous tissue during flexion and rotation of the head and neck. Furthermore, C1 is the thinnest cervical vertebra which consists of a thin ring of bone with a few small projections. On the anterior end of C1, instead of body or centrum, there is a thin band of bone which is the anterior arch, and a small mass on its anterior surface is called the anterior tubercle [9].

C2 - Axis

During the development of the body, C1 merges to the second cervical vertebra C2, called the

axis. This merging produces the prominent dens process of the axis. A transverse ligament attaches the dens to the inner surface of the atlas, which forms a rotation for the atlas and the skull. Lack of a separate ventral body, allows the C1-C2 joint a wide range of lateral movement of the head and neck. Muscles that direct the head and neck position, are linked to the robust spin process of the axis [1, 9].

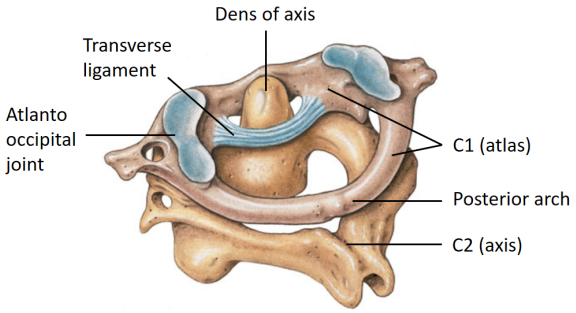

Figure 2.2: The figure shows two upper vertebrae, atlas and axis. Axis' vertebral body is provided with dens, secured in ring-shaped atlas. Atlas has a transverse ligament that keeps the dens in right position. The head rests on atlas, with help from atlanto occipital joints forming joint with atlas. [1, 10]

C3-C6

The C3-C6 vertebrae are categorized as very uniform and have vertebral arch that protects the spinal cord, as well as a centrum or ventral body that provides strength, protection and mobility to the spine thereby to the body. The vertebral body is concave on its upper surface, and convex beneath with cartilage-shaped intervertebral discs, which provides cushioning between these surfaces. The intervertebral discs consist of thin masses of hard fibrocartilage surrounding a center of soft gel, see fig 2.1a. Every single disc has a biomechanical function and behave as a shock absorber, allows impact and motion, and helping to keep the vertebral column positioning. A large vertebral foramen allows flow of the nerves of the spinal cord, see figure 2.3, where the vertebral vein and vertebral artery pass from the spinal column to the body [9, 2].

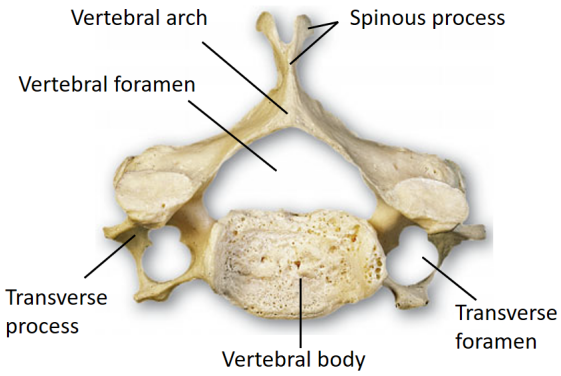

Figure 2.3: The figure shows cervical vertebra with a superior view. This illustrates cervical vertebra of C3 to C6, where the remarkable is the split of the spinous process and the hole in the transverse process, which allows vertebral arteries to provide blood supply to the upper spinal cord, brainstem, cerebellum and posterior part of the brain [1, 10].

C7
The C7 is the most inferior cervical vertebra. It has a long thin spinous process that ends in a wide tubercle, which is the interface between the cervical curve that bows anteriorly, and the thoracic curve that bends posterior, see figure 2.1a. Since transverse processes of C7 are large, they allow an additional surface area for muscle attachment. Elastic ligament starting at the C7 extends to an insertion sideways the occipital crest of the skull. It is attached to the other cervical vertebrae, and when the head is upright, this ligament acts as the cord which holds cervical curvature without muscular action. When the head is flexed, the elastic ligament helps return the head to an upright position [1].

2.1.1 Mobility of Cervical Spine

The cervical spine is much more mobile compared to the thoracic or lumbar regions of the spine [1]. The cervical motion is modelled as a spring-like spine structure with linear joint muscles [5]. The cervical spine in flexion and extension is typically assumed with linear and continuous joint motions [5] with a large range of motion (ROM), see fig 2.4.

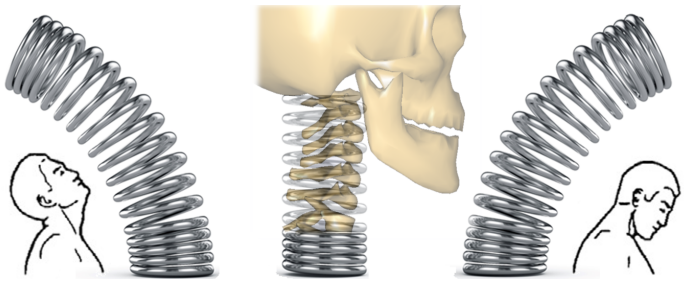

Figure 2.4: The figure illustrates the spring-like spine structure and how the cervical spine is assumed during flexion and extension in the sagittal plane.

ROM is the range of physiologic intervertebral motion measured from the neutral position. It variates and is based on age, gender, body structure etc. [2]. The ROM is articulated as rotation and translation in three planes, where articulation refers to the arching action when the bones interact, wherever they interconnect [1].
As illustrated in fig. 2.5, flexion/extension movement goes from upright position to forward or backward bending. When the head is upright, the ligaments act as a string on an arc that maintains the cervical curve without muscle effort. By forward bending of the neck, the elasticity in the ligament helps the head return to an upright position. The articulation between atlanto occipital condyles and the C1, allows the head flex and extend in a nodding motion [1].

Further extension passing the anatomical upright position is called hyperextension, and takes place when the head bends backwards. The rotational movement happens when C1 articulates with C2 [1]. Since the spinous process of the vertebra is short and the split at the edge sticks horizontally backwards, see fig 2.3, the head can be extended beyond the upright position, without the processes on the cervical vertebrae encountering each other [10].

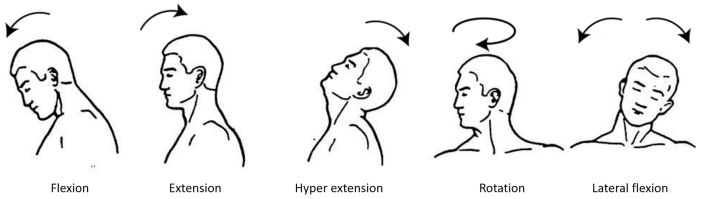

Figure 2.5: The figure shows possible movements of cervical vertebra; flexion-extension, hyperextension, axial rotation and lateral flexion.

2.2 Medical Imaging

There are different medical imaging techniques to visualise the bone and ligament structure of the spine to diagnose the cause of the neck pain. Magnetic Resonance Imaging (MRI) uses strong magnetic field to generate images of the organs in the body. Advantage of MRI of the cervical spine, is the ability to detect a various of conditions of the cervical spine as well as problems in the soft tissue within the spinal column, such as the spinal cord, nerves and disks. MRI can visualise the soft tissue structures directly and separate between various tissues within the spinal canal, without exposing the patient to ionizing radiation. Additionally, MRI can be applied to visualise damage to the spinal cord or nerves as the images are of high quality and can thus provide information that is not found in radiographic images [11, 12].

Computed tomography (CT) scan makes use of differential absorption of X-ray as they pass through the body and form digital matrices which are subsequently converted to cross-sectional images. A CT scan is suitable when imaging complex bone fractures, eroded joints or bone tumours, since it contains more details than conventional X-ray [12]. Furthermore, it provides direct visualisation of the facet joints, intervertebral foramen, neural arches, intervertebral discs, and muscles [11].

Fluoroscopy is X-ray based and the physical principles are similar to the common X-ray image chain, from X-ray beam generation to image display. Video fluoroscopy is a functional examination technique and takes multiple images per second and enables dynamic real-time scans to look at anatomical and functional properties during motion. For that reason, it is an appreciated imaging technology for investigation of intervertebral movements [8].
Previously, video fluoroscopy has been reliably reported for in-vivo studies of spine kinematics by recording the motion of cervical, thoracic, and lumbar region of the vertebrae [13, 14, 7, 15, 6].
For example, [Breen et al., 2012] [7] recorded and analysed the intervertebral motion during fluoroscopy, and [Wu et al., 2007] [16] measured the intervertebral angulation and translation during cervical flexion and extension using video fluoroscopy. A recent study [Wang et al.,2017] has quantified anti-directional cervical joint motion during flexion and extension of the neck, also recorded with video fluoroscopy in healthy subjects [5].

Figure 2.6 shows images of video fluoroscopy scans of the cervical vertebra, where the bone structure is visible when moving from upright position to end-range flexion and extension movements. The images are extracted from fluoroscopy videos obtained from [5].

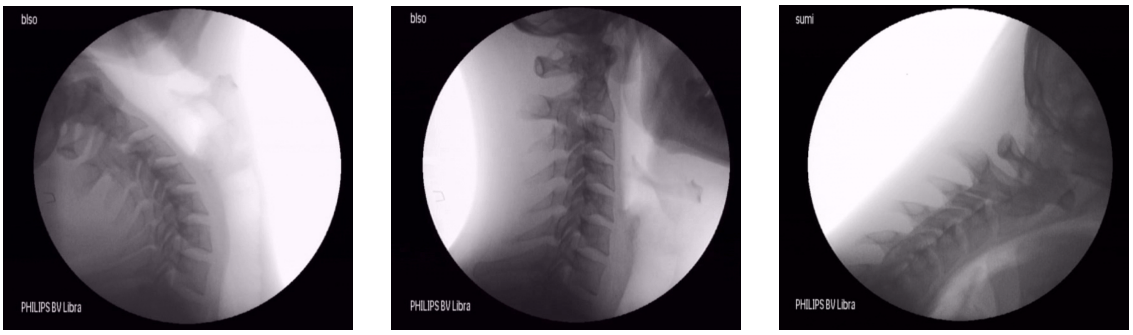

(a) Cervical extension **(b)** Cervical upright position **(c)** Cervical flexion

Figure 2.6: (a), (b) and (c) show images of a healthy cervical vertebra in extension, upright position and flexion, respectively. [5]

2.2.1 Vertebral Tracking

Tracking is the process of estimating how an object (the vertebra) moves during a fluoroscopy sequence between frames [17]. The purpose of vertebral tracking in video sequences, is to obtain time dependent vertebral information through frames.
Within the cardiac imaging field, tracking has been an area of publications for many years. The different principles of tracking an object should remain the same across different anatomical areas [18].
In order to track and locate the vertebrae, segmentation methods like edge detection have been used in image processing. Segmentation is the process of dividing images into constituent subregions which are homogeneous in intensity, texture, depth or color and non-overlapping. The result of segmentation is either an image of each region identified by labels or a set of contours described by region boundaries [19].
When vertebrae are to be tracked, specific requirements are set for which properties to segment. By marking the boundaries, the object detected in the first frame and the object region is iteratively updated during tracking, based on information from previous frames [20, 21].
Manual identification in video sequences has been used for vertebrae tracking [22]. However, in each frame, landmarks must be manually located and inaccurate procedure may cause errors in calculating kinematic parameters. For the measurement of the lumbar spine, [Frobin et al., 1996] developed an accurate method to record and track the spine in the sagittal plane. The method consisted of marking four corners of a vertebrae by an expert and then constructing geometric parameters that described the angle of axial rotation, lateral tilt and off-centre positioning of the vertebrae [22].

In vertebral tracking throughout video fluoroscopy sequence, the functional movement of the cervical spine is acquired [23]. The vertebra is detected in the first frame, and location and region of the vertebrae is iteratively updated during tracking [17]. Fully automatic tracking of the cervical vertebra does not exist yet, however semi-automatic methods have recently been made available [24]. In [Reinartz et al.,2009], a tracking algorithm that could track the skull and cervical vertebra throughout video fluoroscopy recordings was made. The subjects were recorded with 10 frames per second in the sagittal plane from maximum flexion to extension and the method could accurately track throughout the entire video sequence [23]. [Nohr et al., 2017] landmarked the corners of the cervical vertebrae manually depending on the shape. Then, the template was used to compute in all frames to track the cervical vertebrae. Irregularities in tracking was found in the upper cervical vertebra due to the

change of vertebra during motion [24].
In a recent observational study, [Wang et al., 2017] used the flexion and extension movements from neutral to end-rage ROM. Eventually, the videos were divided into 10% epochs with regard to C0/C7 ROM from neutral to end-range positions and found that the cervical spine motion produced anti-directional joint motions [5].

2.3 Intervertebral Kinematics

Functional examination of the intervertebral structure using video fluoroscopy, can be helpful in order to show complications related to neck pain. If no fractures can be observed in a stationary state, recording during motion may contribute to the diagnosis of ligament damage. [Ahmadi et al., 2009] used video fluoroscopy to develop a reliable measurement technique to measure lumbar spine kinematics in patients with lower back pain [25].
Kinematics is the study of measuring and observing motion without taking force and mass into account and intervertebral kinematics is used to describe and quantify the spinal movement [26, 27].

2.3.1 Intervertebral Joint Motion

Despite the established knowledge about the cervical motion, recent studies do not support the linear pattern of joint motion during flexion and extension in healthy subjects. Anti-directional joint motion has been defined as a motion opposite to the expected motion direction [5, 6]. Although, the upper cervical joints (C0-C2) extend, i.e. bend backwards, it has been found that the lower cervical joints (C6-C7) flex, and the other way around, see section 2.3.2. This statement is not applicable to all joints in all healthy individuals, since each joint of each subject has a different characteristic. The anti-directional movement of atlas (C1) has been supported with the biconvex anatomy of the atlanto-axial articulation. Furthermore, the anti-directional motions for C7/T1[1] were also demonstrated [5].

2.3.2 Anti-Directional Joint Motion

In the recent study by [Wang et al., 2017], movements in vertebrae in the opposite direction have been found. Anti-directional joint motion has been defined as opposite motion to the desired motion direction, also called pro-directional. The calculation of each epoch was performed so that the difference in degrees was measured between two adjacent 10% interpolated images. The joint motion angles were divided for each joint from C0/C1 to C6/C7. Two flexion and two extension recordings gave 10 joint motion angles, where repetition of the two flexions and extensions motions became 70 joint motion angles, before calculating anti- and pro-directional joint motion.
The anti-directional C0/C7 motion is the sum of the negative numbers among the 70 joint motion angles, whereas the cervical pro-directional C0/C7 motion is the sum of the positive numbers among the 70 joint motion angles.
As shown in table 2.1, the ratio between anti-directional movements and the pro-motion movement is measured and calculated.
The average C0/C7 ROM for flexion was 51.9 $\pm$ 9.3°, and the total anti-directional ROM for flexion was 39.9 $\pm$ 14.3°. When calculating, this gives that the flexion movement consists of approximately 76.9% of the anti-directional motion. For extension movement, the ratio

[1] T1 is a part of the thoracic vertebrae, located beneath the last cervical vertebra [1]

between anti-directional motion and resultant motion was 71.9%.

	Average C0/C7 ROM	**Anti-directional C0/C7 ROM**	**Pro-directional C0/C7 ROM**
Flexion	51.9 ± 9.3°	39.9 ± 14.3°	91.9 ± 16.3°
Extension	57.3 ± 12.1°	40.2 ± 10.8°	91.9 ± 16.3°

Table 2.1: The table shows the ratio between flexion-extension movements for average ROM and anti-directional ROM within the pro-directional ROM in cervical spine C0/C7. The anti-directional movements constituted 42.8 ± 9.7% of the pro-directional movements for flexion. The ratio between anti- and pro-directional motions is 41.2 ± 8.2% for extension.

Furthermore, the upper cervical joints (C0/C1, C1/C2, C2/C3) showed to have a greater ratio of anti-directional movements compared to the lower cervical joints (C4/C5, C5/C6, and C6/C7). This means that the joints C1/C2 and C2/C3 have greater anti-directional movements in a pro-directional movement.

2.4 Predictive Analysis

Prediction is used to determine observations based on selected features. Regression analysis estimates the relationship among variables and is widely used for predicting outcomes. When predicting the outcome, a training data set must be used to train the features. By using the training on known data, a prediction model can be build. After the model has been trained, it can be tested and then evaluated. A model must meet some criteria to be identified as good. The performance of the model can be evaluated by testing how accurate it can predict. The sensitivity of the model can be tested by looking at the number of positive predicted values that are correctly positive predicted. When testing for specificity, the number of negative predicted values that are correctly negative predicted is tested. High sensitivity and specificity indicates the predicted model as good [28, 29].

There has recently been made an predictive analysis of muscle forces on the cervical spine. Using the biomechanical approach, [Abbeele et al., 2017] selected six different components, including different forces that could affect the muscle movement in the cervical spine. The prediction outcome was considered valid, as it was consistent with the available literature [30]. Another study [Ritter et al., 2003] used various regression analysis methods to predict the flexion-extension ROM of the knee [31]. [Hahne et al., 2004] used regression analysis to predict the appearance of lower back pain [32]. A prediction of the cervical spine movement does not exist in the literature.

3 | Project Aim

In order to provide an option for clinical diagnosis of neck pain, measurements of the intervertebral kinematics can be used to evaluate the movement of the cervical spine by performing functional examination. Motion of intervertebral kinematics is used to gain a better understanding of the movement to ease neck pain and general back pain.

3.1 Research Statement

Manual segmentation and tracking of vertebral areas in video sequences is a cumbersome and time-consuming process. Several semi-automatic methods have been developed, but the template process requires detailed landmarking of each vertebrae in the first frame. It was also reported to be difficult to track throughout the video sequences at upper and lower vertebrae, due to the vertebral locations behind the skull and shoulder.

Motion in the cervical vertebrae in the opposite direction, are called anti-directional joint motion. Since the anti-directional movement is a new research field, the categorisation of the anti-directional ROM has not been made. The acuity of the anti-directional joint motions in healthy subjects is important. This is due to the cervical spine motion in healthy subjects function as baseline for treatment options for patients with neck pain disorders. Uncategorised ROM of flexion-extension movement of the cervical spine, can lead to misdiagnoses and wrong treatment.
Categorisation of the cervical joint motion pattern in regards to anti-directional does not exist. The cervical spine motion pattern is expected to be categorised into specific groups depending on the variation of ROM. By categorising motion patterns into similar groups, it enables the clinicians with a better biomechanical information for diagnosis and rehabilitation of anti-directional motion.
A statistical approach to predict the cervical spine motion does not exist yet.

3.1.1 Problem Statement

Due to change of shape during motion, the upper vertebrae "C0/C1" was found to be challenging to segment in vertebral tracking approaches. Based on current knowledge of acquirement of the rotation of cervical vertebrae and the irregularities in the upper vertebra when tracking, a problem statement was set:

How can the rotational movements of the seven joints of the cervical vertebrae ("C0/C7") be predicted during flexion and extension? Are there any of the seven joints that are more characteristic in order to predict rotations of the upper vertebra?

To answer the problem statement, two aims were identified. The first aim was to predict every single cervical joint's maximum rotation in healthy subjects, and then analyse if statistical differences occurred between manually measured rotations compared to predicted rotations.

Aim 1: Predict the full range flexion-extension rotations of each cervical vertebra and investigate whether there are more distinctive joints to predict upper vertebra.

After predicting the flexion-extension rotational movement of each vertebra, the second aim was to investigate the whole ROM in regards to anti-directional joint motion and possibly categorise the maximum ROM into distinctive subgroups of similar motion pattern. Categorisation opens up for comparable possibilities of intervertebral motion patterns in healthy subjects. The goal is to obtain the opportunity to group patients into subgroups with various neck pain, to establish better treatment options.

Aim 2: Division of participants into distinctive subgroups of similar cervical ROM patterns, in flexion and extension movement.

3.1.2 Solution strategy

The predictions of cervical vertebrae was carried out by using multiple linear regression analysis. For the division of participants, cluster analysis approach was used. All detailed descriptions of methods are explained in Chapter 4 in Materials and Methods. The solution strategy is divided into three parts, of which:

Part 1: Prediction using six cervical joints: A prediction of the complete cervical motion, by using all cervical joints as predictors in multiple linear regression analysis.

Part 2: Prediction using two cervical joints: A prediction of the flexion/extension motion in the uppermost joint "C0/C1" using only two characteristic joints ("C3/C4" and "C4/C5") as predictors.

Part 3: Division into subgroups of motion pattern: Divide the data into two separate groups of distinct motion patterns in order to provide treatment options depending on information of the subgroup.

4 | Materials and Methods

This chapter is divided into three parts. The first part is based on the prediction of the total rotation in all joints, using six vertebrae as predictors. Selected methods and approaches for prediction of flexion and extension are outlined in figure 4.1. A description of the chosen methods follows the direction of arrows in the figures.

In the second part, two vertebrae have been used to predict the total rotation in the upper cervical vertebra "C0/C1". In this part, the same figure 4.1 is used to describe the prediction approach, with the only difference that fewer parameters were used.

In part three, the figure 4.2 shows the calculation for observed and predicted data set, with associated clustering into two groups for flexion and extension. The method of division of the groups in similar joint motion pattern is described in section 4.3.

Part 1: Prediction using six cervical joints and
Part 2: Prediction using two cervical joints

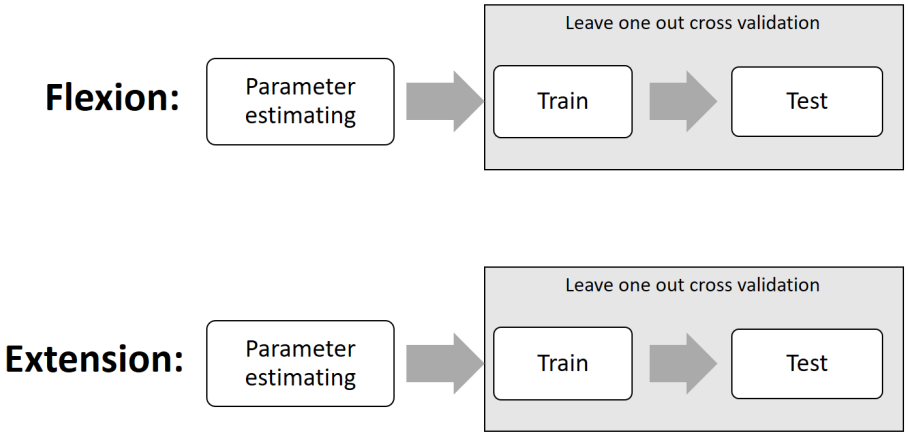

Figure 4.1: This figure shows the selected methods for prediction of flexion and extension in Part 1 and Part 2.

Part 3: Division into subgroups of motion pattern

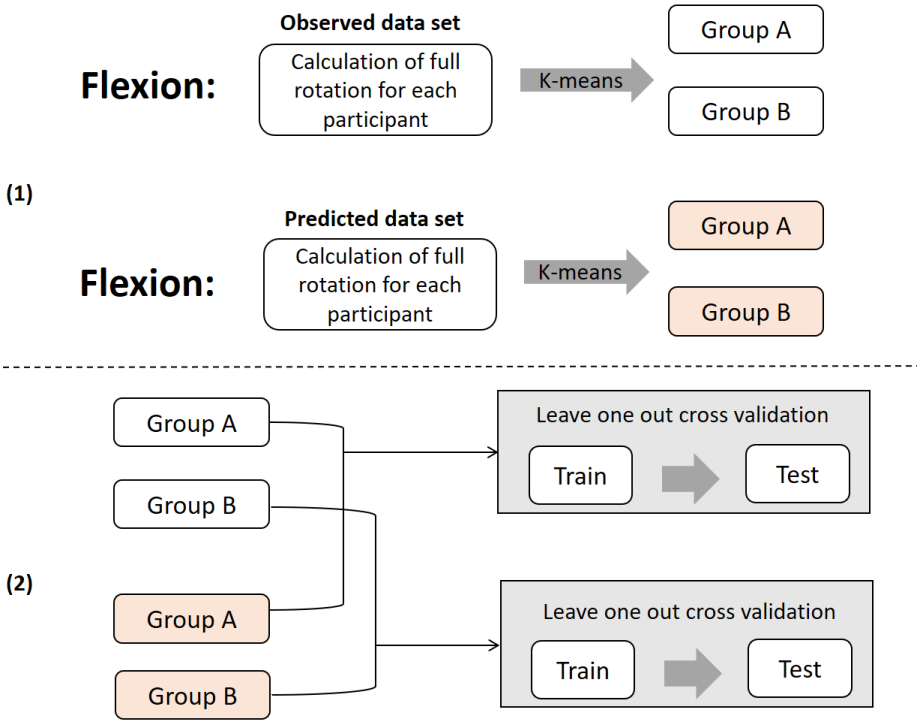

Figure 4.2: This figure shows part 3, where (1) indicates the method of clustering into two groups A and B. (2) shows the validation process for each group. This approach was done for flexion and extension.

4.1 Study Data

The available data for this project was obtained by Chiropractor Niels Peter Bak Carsten at Vejgaard Kiropraktisk Klinik, Aalborg, Denmark. In collaboration with Center for Neuroplasticity and Pain (CNAP), supported by the Danish National Research Foundation (DNRF121), the data was derived from Wang et al., which is an observational study investigating the healthy cervical flexion and extension in anti-directional motion [5].

The data consists of fluoroscopy videos of the cervical spine, recorded from the left side with 25 frames per second, with the source-to-subject (C7) distance of 76 cm (Philips BV Libra, 2006, Netherland), with 45 KV, 208 mA, 6.0 ms X-ray pulses. The average radiation exposure was estimated to be 0.48 mSv (PCXMC software, STUK, Helsinki, Finland) [5].

A total of 33 healthy participants (12 females and 21 males) were enrolled, where one was excluded from the extension category. Thus, N = 33 in flexion, N = 32 in extension. All participants performed flexion and extension motions from neutral to end-range when sitting in a chair with knees, hips and ankles at 90°. Shoulders, elbows and waist were locked with straps. Participants had custom made glasses on with external markers to be able to better visual tracking of the occiput. For demogprahic factors, see fig. 4.3.

	Males (21)	Females (12)
Age (years)	27.0 ± 5.3	23.8 ± 3.0
Height (cm)	179.0 ± 8.4	164.4 ± 7.9
Weight (kg)	73.7 ± 9.7	61.2 ± 12.6
BMI (kg/m^2)	22.9 ± 1.8	22.5 ± 2.9

Figure 4.3: The table shows general mean and ± std characteristics of the participants. BMI indicates body mass index.

Examination protocol

Participants were instructed to visually follow a line on the floor, wall, ceiling, and a cross at eye height (natural position). For each participant, two videos were recorded: one while the subject performed a flexion movement, and one during an extension movement. Flexion and extension motions were free and unlimited. Compliance to flexion or extension motion speed of 12 seconds was practiced before recording. Steady neutral and end-range positions were recorded for 2 seconds.
After the end-range recording, participants returned to the neutral position at their own pace. The fluoroscopy videos were divided into 10% epochs of "C0/C7" range of motion (ROM), where pro-directional and anti-directional motions in each 10% epoch were extracted. This gives a total of 70 joint motion angles, in both flexion and extension, see fig. 4.4. The ratio between anti-directional motion with respect to pro-directional motion, was calculated for joints and 10% epochs, where 0% is equal to no anti-directional movement [5].

Data overview

This data is summarised where data shows the total movement from the upright position to the actual epoch. Data is accumulated so that full movement in either flexion or extension direction starts from 10% and is completed at end-range, 100%. The seven joints are characterised by "C0/C1", "C1/C2" up to "C6/C7". Positive numbers show the joint opens in intended direction, negative numbers show that the joint opens in anti-direction, see fig. 4.4. The example shows the accumulated motion in each of the 10 epochs from 10% to 100%. The rotations are calculated in degrees.

	ROM C0/C7	Accumulated motion								
Segments	10%	20%	30%	40%	50%	60%	70%	80%	90%	100%
'C0/C1'	10,3029	13,0459	15,0252	17,2888	22,0712	21,5751	21,5883	25,4746	24,6746	24,5889
'C1/C2'	-1,94526	-2,41906	-2,4115	-0,53048	-6,7377	-2,55136	-3,92642	-3,4396	-3,58784	-5,0789
'C2/C3'	-2,43638	-0,87939	-2,81494	-3,12593	-1,49261	-3,99609	-1,23516	-4,74265	-2,34235	-2,643
'C3/C4'	2,20523	0,31422	2,84488	2,73809	4,65303	2,16537	2,75681	5,66306	4,64648	4,3788
'C4/C5'	-2,19326	2,92446	3,72472	2,78595	3,9102	7,00135	6,47023	6,16009	7,54798	10,7034
'C5/C6'	-0,66111	-1,45742	-2,12385	1,80194	4,41276	8,97926	11,7616	13,5955	14,3793	13,9201
'C6/C7'	0,42023	-0,14405	2,83253	1,811	1,64491	0,98052	2,43109	2,82779	5,91301	11,0542

Figure 4.4: Data of a single participant when performing extension. The figure shows every single rotation of the joint, in every epoch. The last epoch 100% shows the maximum cervical spine movement for every joint.

To be accepted as a healthy participant, the exclusion criteria were:

Exclusion criteria

- Neck pain within 3 months

- Any neck disorders
- Cervical trauma
- Possible pregnancy
- Rheumatoid arthritis
- Other inflammatory disorders

Prediction using six cervical joints & Prediction using two cervical joints

4.2 Statistical Analysis

Two available data sets for flexion and extension were given for 33 participants, where the given data sets are normally distributed. In this report, all statistical analysis was conducted using MATLAB2017. The aim of using statistical analysis, was to predict the motion of all vertebrae and one specific vertebra by analysing the movement of others.

4.2.1 Multiple Linear Regression

Multiple linear regression (MLR) is an extension of simple linear regression analysis. MLR is a method which describes the relationship between a dependent variable (Y) and a number of independent explanatory variables (X_1, X_2,...X_k). This method is carried out to predict the values of a dependent variable Y, given a set of variables X_k (See figure 4.5). Compared to a simple linear regression for a population, in MLR, Y is considered dependent upon more than one variable [28].

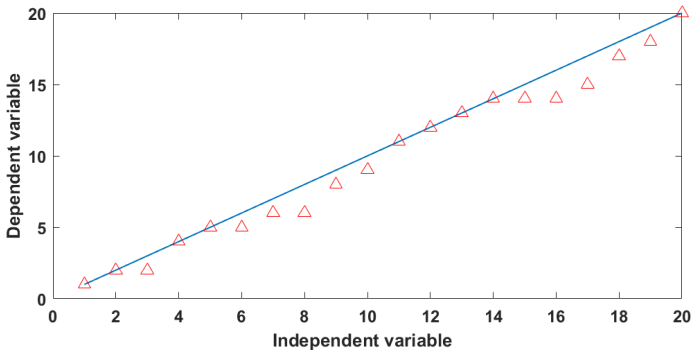

Figure 4.5: The figure illustrates a dependent variable relationship (Y) to independent variables (X_k). If a point lies on the fitted line exactly, then its deviation is 0.

When Y is linear dependent on more than one independent variable, X_k, the value of α is the value of Y when all independent variables are set to zero, see equation 4.1.

$$Y = \alpha + \beta_1 X_1 + \beta_2 X_2 + \beta_3 X_3 + ... + \beta_k X_k \tag{4.1}$$

Y is the predicted value, α is where the line crosses the y-axis (Y-intercept), β is the regression coefficient where β_1 is the change in Y for each 1 increment change in X_1, and β_2 is the change in Y for each increment change in X_2 etc.

The aim of using MLR, was to 1) predict the motion of all vertebrae and 2) predict one specific vertebra by analysing the movement of others. Hence, this statistical approach was considered suitable, as it allows analysing movement of other vertebrae, where a prediction of the motion (dependent variable Y) can be performed.

Assumption
In this model, it is assumed that there is a linear relationship between the predicted dependent variable and the independent variables. The second assumption is already given, as it was informed that the data sets were normally distributed in advance. When there is high correlation between the independent variables, multicollinearity can occur in the model, hence, a third assumption is that there is no multicollinearity in the model. The last assumption is that independent variables $X_1 ... X_k$ must not be linearly dependent on each other.

4.2.2 Estimates of the Model Parameters

To answer part 1), all 10 epochs were trained for each joint, where regression coefficients for all seven joints were found. Then, the regression coefficients were inserted into the equation 4.1. Six independent variables (X_{1-6}) representing six cervical vertebra joint motions, were used to find the last desired joint motion Y. For each participant, this was repeated seven times, i.e, for each cervical vertebra from C0/C7. In the end, all joints' 10 epochs for motion was predicted.

The model allows to investigate how a set of explanatory variables are associated with dependent variables of interest.
To answer part 2) the request of fewer joints as predictors, the number of independent variables were reduced. By using two predictors to find a third joints' motion, two independent joints (X_1) and (X_2) were inserted in the equation 4.1.

To solve the second part, a prediction of the upper vertebra "C0/C1" motion, joints "C3/C4" and "C4/C5" were chosen as predictors, hence as independent variables (X_1) and (X_2), respectively. All 10 epochs for joint "C3/C4" and "C4/C5" were trained, and by using joint "C0/C1" as the independent variable Y, regression coefficients for this joint were found. Inserting the coefficients into equation 4.2, resulted in predicting the motion of joint "C0/C1".

$$Y = \alpha + \beta_1 X_1 + \beta_2 X_2 \tag{4.2}$$

4.2.3 Training and evaluation

There are many approaches to test for generalisability, here among a hold out cross validation (CV), k-fold CV and leave one out CV (LOOCV). The hold out CV relates to only training the data with a subset of the total data, and then tests the model with the data not used for training. In k-fold CV, a single subsample k is held as the validation data for testing the model, where the remaining *k-1* are used for training the data. This process is repeated k times. LOOCV is an option where all data, but one sample, is used to train the model, and it is then tested with the lone sample, which is done for every sample. The training data set consists of n-1, and test data set consists of 1, where n is total data. Therefore, the number

of iterations for the training and testing process is equal to the number of data elements. [33, 34]
In this study, the LOOCV divided the data into group for test (1) and a group for training (32). This iteration was repeated until all participants was used for test, and the results were validated in LOOCV.

Model Validation

The degree of relation between the independent and dependent values is determined by coefficient of determination R^2 (R-squared). R^2 represents the amount of variation in the predicted values that can be explained by the model. In a multiple regression model, the R^2 coefficient indicates the proportion of the total variance in the dependent variable Y, explained by independent variables (X_1, X_2,...X_k), e.g. how much variance in Y, is explained in the model. R^2 ranges from 0 to 1, closer the R^2 value is to 1, the better predictive result [28].

$$R^2 = \frac{variance\,of\,predicted\,values\,(\hat{y})}{variance\,of\,observed\,values\,(y)}$$

($\hat{y}$) is the predicted value, and (y) is the observed value.

Since R^2 indicates how much variation is explained in the model, an 0.95 R^2 means the model explains 95% of variation within the data. Greater R^2, the better the model.

In order to validate the developed models in Part 1 and Part 2, the variance of the predicted values of rotation, and the variance of the observed values of rotation were found. In this manner, the R^2 values for each joint were calculated.

R^2 alone cannot be used to help validating a model, therefore, a root mean squared error (RMSE) was calculated to show model performance. RMSE measures how much error there is between two data sets by comparing the predicted and observed values. RMSE is the standard deviation of the residuals, e.g. prediction errors. Residuals are measurements of how far from the regression line the data points are, also the difference between predicted and observed values [28].

$$RMSE = \sqrt{\frac{\sum_{i=1}^{n}(\hat{y}_i - y_i)^2}{n}}$$

Where $\sum$ sums up the differences between $\hat{y}_i$, the predicted value, and y_i, the observed value, in square. n is the total sample size.
For a reasonable fit, the RMSE to predicted and observed variation must be similar.

Division into subgroups of motion pattern

4.3 Division of Motion Pattern

In regard to answer aim 2 of the problem statement, a categorisation of the participants' full neck movement was made. In order to provide treatment options depending on information of the subgroup, the data was divided into two separate groups of distinct motion patterns.

The flexion-extension movement was divided so that both observed study data and predicted rotations were grouped into two, respectively group A and group B.

The maximum motion for flexion and extension direction was calculated for each participant. By adding row 100% for each joint, from "C0/C1" to "C6/C7", the maximum rotation was calculated, see fig. 4.6 for an example of 1 random participant. In epoch 100%, the area of calculation of the total ROM is marked with red. This iteration continued until all the participants' total ROM was calculated in the observed study data, and in the predicted data set.

	ROM C0/C7			Accumulated motion						
Segments	10%	20%	30%	40%	50%	60%	70%	80%	90%	100%
'C0/C1'	10,3029	13,0459	15,0252	17,2888	22,0712	21,5751	21,5883	25,4746	24,6746	24,5889
'C1/C2'	-1,94526	-2,41906	-2,4115	-0,53048	-6,7377	-2,55136	-3,92642	-3,4396	-3,58784	-5,0789
'C2/C3'	-2,43638	-0,87939	-2,81494	-3,12593	-1,49261	-3,99609	-1,23516	-4,74265	-2,34235	-2,643
'C3/C4'	2,20523	0,31422	2,84488	2,73809	4,65303	2,16537	2,75681	5,66306	4,64648	4,3788
'C4/C5'	-2,19326	2,92446	3,72472	2,78595	3,9102	7,00135	6,47023	6,16009	7,54798	10,7034
'C5/C6'	-0,66111	-1,45742	-2,12385	1,80194	4,41276	8,97926	11,7616	13,5955	14,3793	13,9201
'C6/C7'	0,42023	-0,14405	2,83253	1,811	1,64491	0,98052	2,43109	2,82779	5,91301	11,0542
										56,9235

Figure 4.6: The figure shows an example of a single participants' full rotational neck movement in extension. As outlined on the figure, the full rotation is calculated to 56,9235°.

After calculating the total ROM of each participant, cluster analysis approach was used to group these. This clustering method was carried out by k-means function, which aims to partition total observations into k clusters, where each observation belongs to the cluster with the nearest mean. In that way, it forms homogeneous clusters and segments the data so the variation is minimised [33].

In this study, clustering was performed using the total ROM in flexion and extension, where k was set to 2, $k=2$, hence, two subgroups of each movement was initialised.

In figure 4.7 and 4.8, the groups are illustrated for flexion and extension with the associated subgroups. Figure 4.7 shows the clustering of the observed study data, and figure 4.8 shows the clustering of the predicted data set.

Observed study data

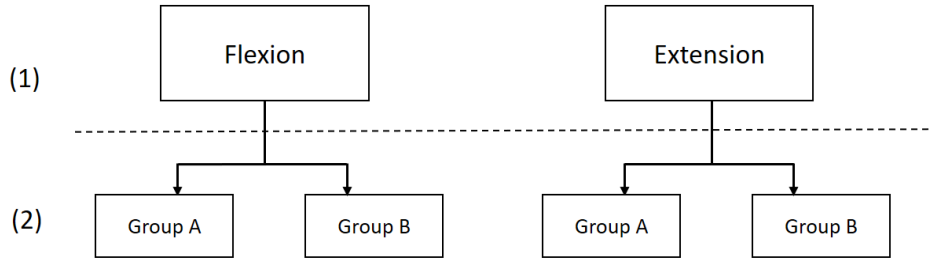

Figure 4.7: The figure illustrates (1) initial groups flexion and extension of observed study data, where (2) shows the initialised subgroups after k-means partition of ROM for flexion and extension.

Predicted data set

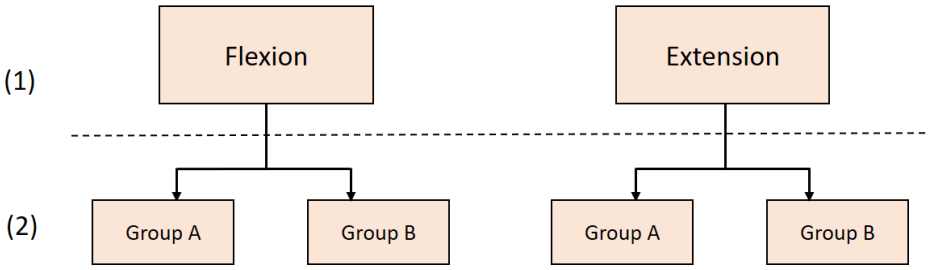

Figure 4.8: The figure illustrates (1) initial groups flexion and extension of the predicted data set, where (2) shows the initialised subgroups after k-means partition of ROM for flexion and extension.

After division of total ROM of flexion and extension into subgroup A and B, the subgroups were first trained and then tested with LOOCV.

Cross validation between the observed study data and predicted data set was made, where the mean R^2 and mean RMSE was calculated for all four subgroups. Since the goal of division of motion pattern, was to provide clinical options depending on distinct motion pattern, the correlation between subgroups: (Observed Flexion A,Predicted Flexion A), (Observed Flexion B,Predicted Flexion B), (Observed Extension A,Predicted Extension A) and (Observed Extension B,Predicted Extension B) was carried out to be able to compare the observed study data and the predicted data set. This was in regard to test the quality of the rotations in the predicted data set, against the observed study data.

It is known that 40% of the pro-directional motion contains anti-directional movement in the total ROM. In case the motion pattern of the same participant were clustered into two different subgroups for the observed study data and predicted data set, these participants were excluded in order to make a valid evaluation.

5 | Results

In this chapter the results are divided into three parts. 1) Prediction of the complete cervical motion by using all cervical joints as predictors. 2) Prediction of a single joint "C0/C1" by using two characteristic predictors "C3/C4" and "C4/C5". 3) Results of divided data of groups with similar joint motion pattern .

Results from all predicted rotations are presented and evaluated in comparison with the manual measured rotations. Only selected participants are shown as examples.

Prediction using six cervical joints

5.1 Evaluation of the Regression Model

Evaluation of the regression model is shown by examples of strong and poor predictions, and is presented in the following sections. The corresponding coefficient of determination (R^2) and root mean squared error (RMSE) values for two groups of data sets, flexion and extension, are also included. Various joints have been used as predictors, where these are outlined in the figure caption.

Graphs are illustrated with observed and predicted rotations for three selected participants in each group, respectively in flexion and extension, one with a good coefficient of determination and one with a lower coefficient of determination . Since an R^2 value near 1 indicates that the independent variable explain most of the variability in the dependent variable, an R^2 value at 0.95 can be described as 95% correlation, which is considered as well predicted. Weak prediction indicates that the fit is not much better than the model. RMSE value for every joints' maximum rotation is also calculated, where the RMSE has the same unit as the dependent variable, e.g. degrees.

5.1.1 Cervical Flexion

In this section, examples of results from the predicted flexion movements are demonstrated. Table 5.1 shows R^2 and RMSE values for each joint, where the correlation between observed variables and predicted variables is calculated. When using all joints as predictors in flexion, the best correlation was seen for joint "C0/C1" with a 98% correlation with the observed data set.

	C0/C1	**C1/C2**	**C2/C3**	**C3/C4**	**C4/C5**	**C5/C6**	**C6/C7**
R^2	0.98 ±0.002	0.97 ±0.002	0.93 ±0.004	0.95 ±0.002	0.95 ±0.001	0.95 ±0.001	0.93 ±0.002
RMSE	0.55 ±0.010	0.94 ±0.019	0.94 ±0.014	0.80 ±0.012	0.85 ±0.011	0.95 ±0.012	1.13 ±0.014

Table 5.1: Mean R^2 and mean RMSE in flexion movement for all seven joints in all 33 participants, where ± is the standard deviation.

In figure 5.1 and 5.2, the predicted rotation model is compared to the measured rotation, in six different participants with weak and strong predictions, respectively. The graphs illustrates the difference rotations between the predicted and observed joint "C6/C7".

Figure 5.1 illustrates examples of how the predicted (red) model follows the observed (blue) rotation in each epoch. It is visually clear that the predicted rotation follows the original rotation in each epoch. Thus, at high and very varying peaks, the predicted model is not precisely predicted in each epoch. An example of this issue occurs in 5.1 (a) and (b). In 5.1 (c), the regression predicts well until epoch 4 and is inaccurate afterwards, after which it again predicts well from epoch 7 to 8. In 5.1 (d), the epochs are predicted so that the regression assumes very varied increase and decrease in epochs, even though the original rotation is not. From epoch 7, the predicted rotations are close to the original.

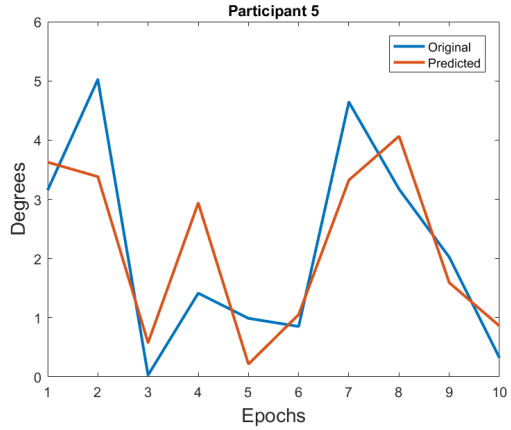

(a) Predicted flexion for participant number 5.

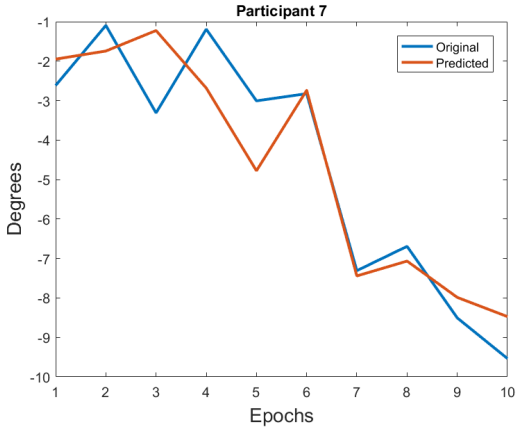

(b) Predicted flexion for participant number 7.

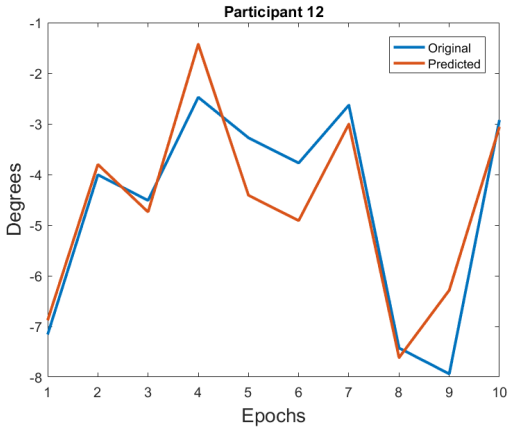

(c) Predicted flexion for participant number 12.

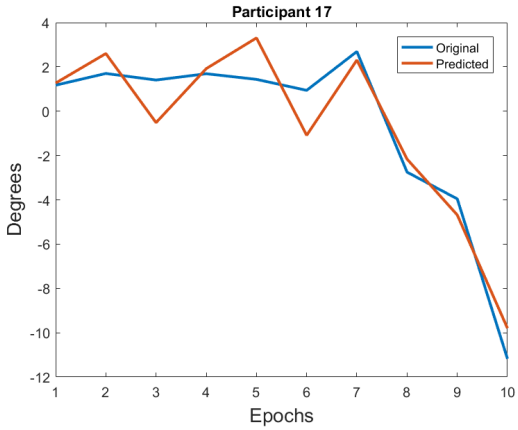

(d) Predicted flexion for participant number 17.

Figure 5.1: (a), (b), (c) and (d) illustrate the poorly predicted flexion rotations of joint "C6/C7"; four participants are shown as example.

In figure 5.2, examples of well predicted flexions of final joint "C6/C7" are illustrated in four different participants. In general, the predicted epochs go in the same direction as the original epochs though increase and decrease in the rotational degrees. The challenge is clearly seen in fig. 5.2 (c), where the predicted regression does not assume the appearance of such rotational changes between epoch 2 and 4. However, the predicted rotation still follows the original rotation.

Figure 5.2: (a), (b), (c) and (d) show examples of strongly predicted flexion rotations in joint "C6/C7".

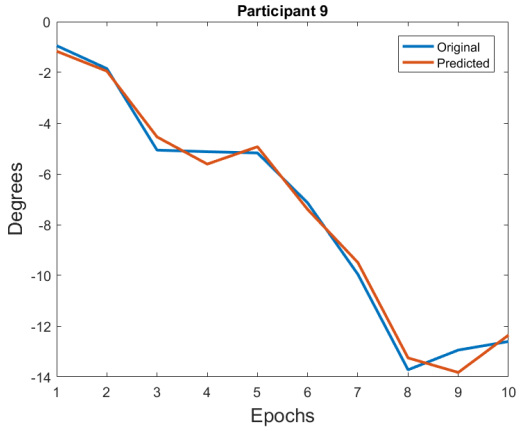

(a) Predicted flexion for participant number 9.

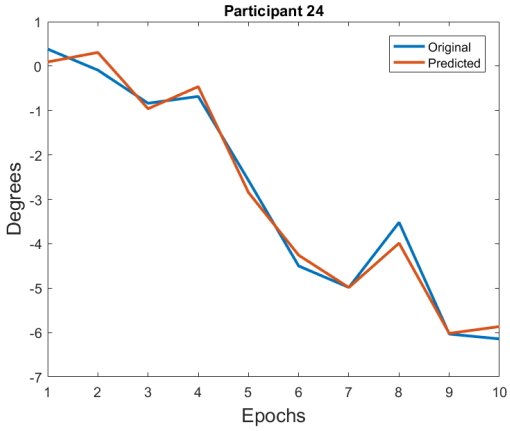

(b) Predicted flexion for participant number 24.

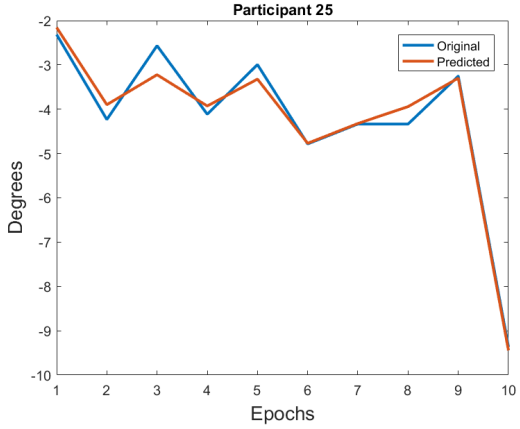

(c) Predicted flexion for participant number 25.

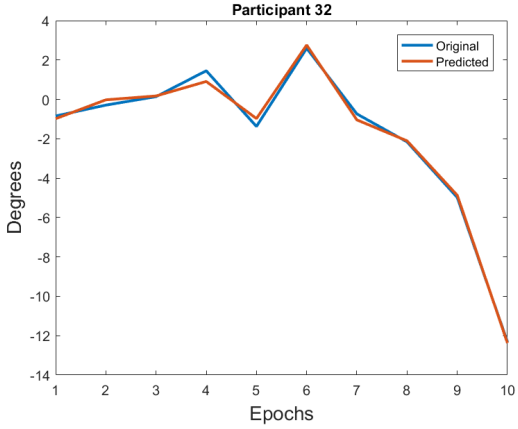

(d) Predicted flexion for participant number 32.

5.1.2 Cervical Extension

In this section, examples of results from the predicted extension movements are demonstrated.

Table 5.2 shows the R^2 and RMSE values for all seven joints. On the examples in the following, only graphs from joint "C6/C7" are demonstrated.

	C0/C1	C1/C2	C2/C3	C3/C4	C4/C5	C5/C6	C6/C7
R^2	0.97 ±0.002	0.95 ±0.003	0.97 ±0.002	0.95 ±0.001	0.96 ±0.001	0.96 ±0.001	0.95 ±0.002
RMSE	1.13 ±0.031	1.03 ±0.039	0.77 ±0.012	0.98 ±0.026	0.85 ±0.013	0.81 ±0.016	0.75 ±0.014

Table 5.2: Mean R^2 and mean RMSE in extension movement for all joints in all 32 participants, where ± is the standard deviation.

In fig. 5.3, four participants' poorly predicted extension rotations are illustated. The predicted and original rotations differ a lot in precision, which is clearly evident in the four figures. In (a), the steep decline in epoch 3 is not predicted, however, except from epoch 7, the pattern nearly follows the original rotations after epoch 5. In (b), the steep descent in epoch 5 is not predicted and the predicted rotation also differs in epoch 7, even though epoch 6 is a correct fit. However, the rotations from epoch 8 to 10 are precisely predicted. In figure (d) and (c), the regression fails to predict after epoch 5. In both graphs, the prediction goes in the opposite direction compared to the original rotation.

Figure 5.3: (a), (b), (c) and (d) show examples of poorly predicted extension rotations.

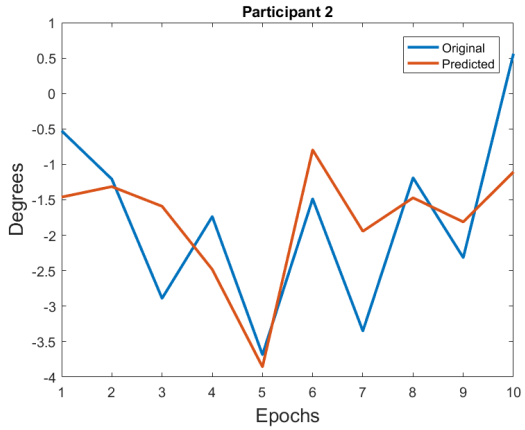

(a) Predicted flexion for participant number 2.

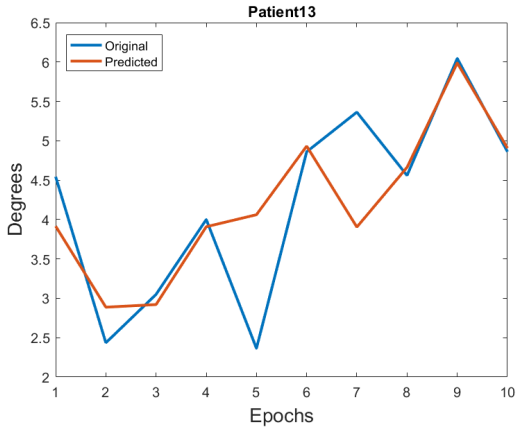

(b) Predicted flexion for participant number 13.

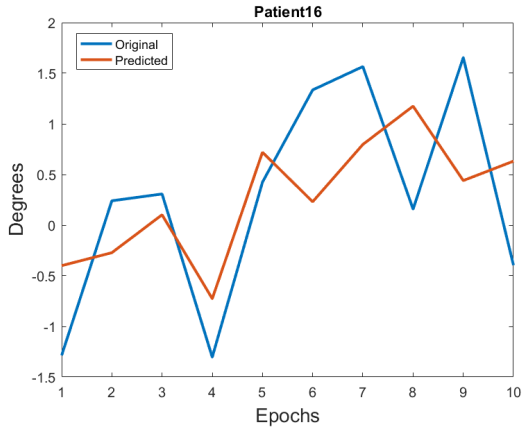

(c) Predicted flexion for participant number 16.

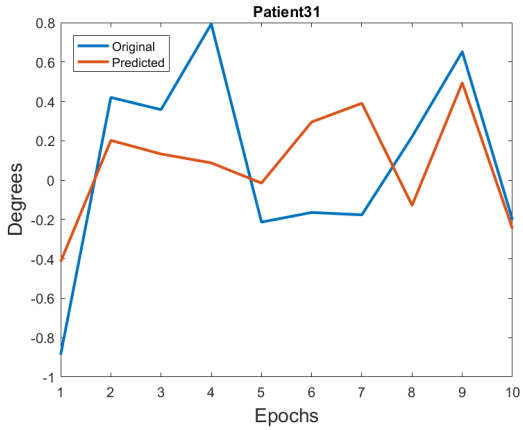

(d) Predicted flexion for participant number 31.

Figure 5.4 shows examples of four participants with well predicted rotations, with small variations throughout the epochs. Although the regression almost predicted all rotations, the short increases and decreases in rotations are sometimes not precise. The challenge is visible in figure (a) and (b) epoch 7, and epoch 2 and 7 in (d). In figure (c), the variations are larger than in the others. In epoch 2, the rotation is predicted as positive, whereas the original is approximately below zero. However, generally, the prediction pattern follows the same pattern as in the original rotations.

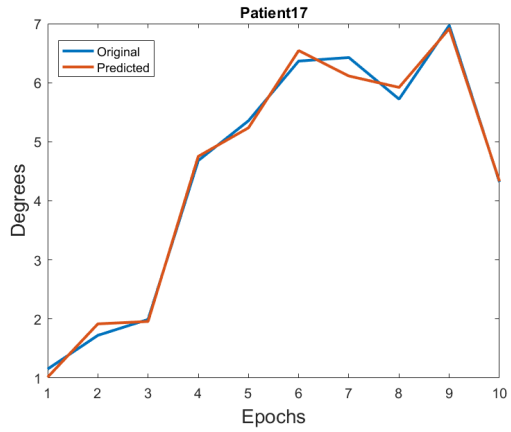

(a) Predicted flexion for participant number 17

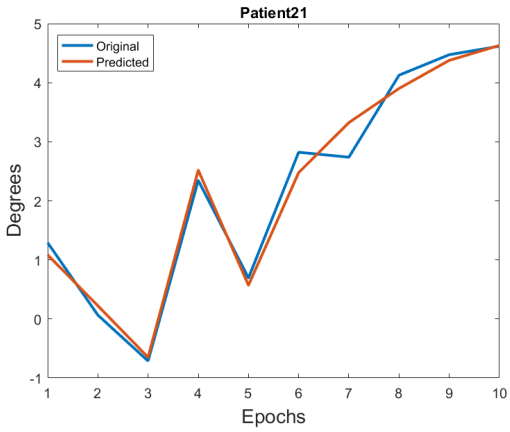

(b) Predicted flexion for participant number 21.

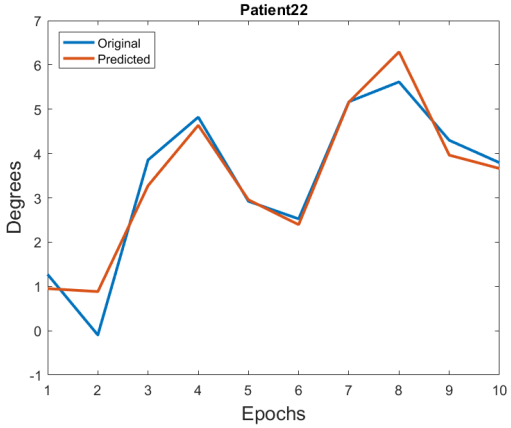

(c) Predicted flexion for participant number 22.

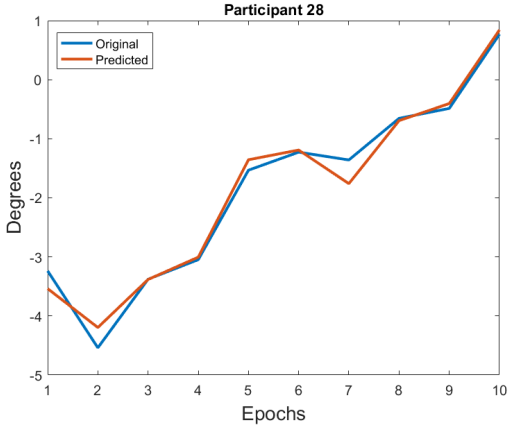

(d) Predicted flexion for participant number 28.

Figure 5.4: (a), (b), (c) and (d) show images of strongly predicted flexion rotations. Predicted degrees (red) are compared to the original degrees (blue).

Prediction using two cervical joints

5.1.3 Evaluation of the Regression Model

This section belongs to part 2, where the result of the regression model with two predictors are described below.
To be able to investigate if a set of fewer joints instead of six, could be assumed as characteristic predictors, joint "C3/C4" and "C4/C5" were used as independent variables in mutiple linear regression. "C3/C4" and "C4/C5" were selected as the most characteristic, as they are localised in the middle of the cervical column and therefore, easily accessible to track during motion.
The two predictors were applied to see the possibility of predicting rotations of joint "C0/C1", since this joint changes shape during motion, thus it is challenging to track with segmentation approaches. To be able to predict "C0/C1", only the independent variables "C3/C4" and "C4/C5" joints were used in the training and testing set. All other joints were not taken into consideration.

In order to demonstrate the outcome, examples of strong and poor predictions by plots and bar graphs are illustrated. Bar graph was chosen to demonstrate positive-negative (±) ratio between the two data sets.

Table 5.3 shows the calculated R^2 and RMSE values in joint "C0/C1" for all 33 participants in flexion. By using two joints as predictors, the correlation between the observed and predicted rotation was calculated to 90%.

	'C0/C1'
R^2	0.90 ±0.01
RMSE	1.25 ±0.02

Table 5.3: The table shows R^2 and RMSE value with mean ± std for flexion.

Prediction of "C0/C1" in Flexion

In figure 5.5 and figure 5.6, the flexion movements demonstrate weak predicted rotations in joint "C0/C1". On both graphs in figure 5.5, the predicted and original rotations for a single participant are illustrated. On the left side, the rotation pattern of both observed and predicted can be seen. The decrease from epoch 6 to 7, from almost 1° to -0.6°, confuses the regression model, and the increase from epoch 7 to 8 is not taken into account. On the bar graph on the right side in figure 5.5, the ± ratio is wrong predicted in 2 out of 10 epochs. Except from epoch 5 and 7, rest of the rotational degrees are also poorly predicted.

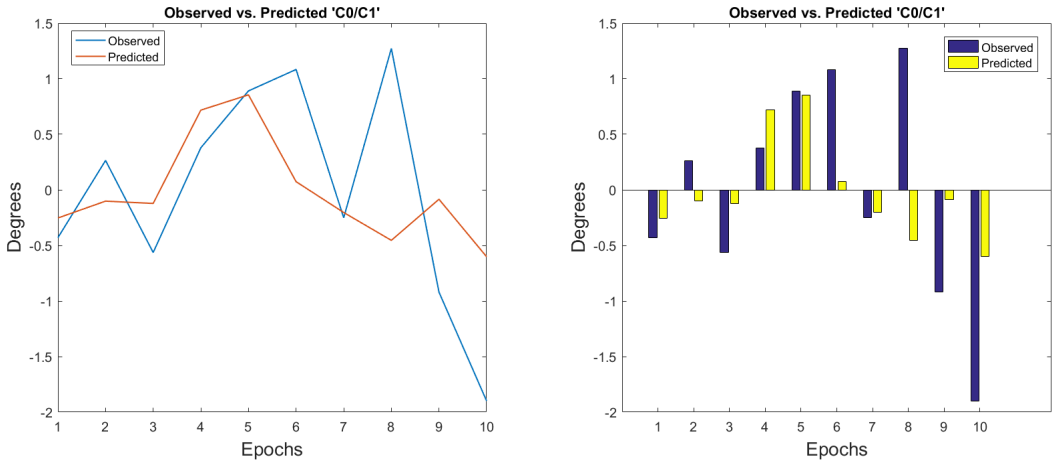

Figure 5.5: Example of weakly predicted joint rotation in flexion. The two figures show the full motion in "C0/C1" in participant number 5. The left side shows the plot of the data. On the right side, the bar graph from exact same movement is illustrated.

In figure 5.6, the entire rotational motion is predicted incorrectly from start to the end. Already in the first epoch, the rotation is mispredicted and cannot correct future predictions in the same joint. On the corresponding bar graph on the right side, the different rotational degrees are very clear. When looking at the ± ratio, all degrees are found in the correct sign. However, this might be useless if the predicted rotations do not tell anything about the movement.

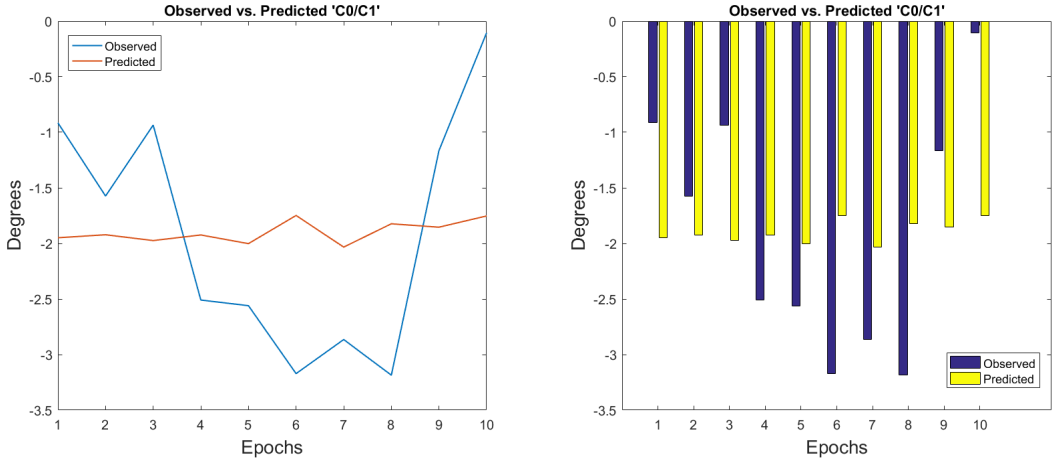

Figure 5.6: Example of weakly predicted joint rotation in flexion. The two figures show the full motion in "C0/C1" in participant number 19. The left side shows the plot of the data. On the right side, the bar graph from exact same movement is illustrated.

In figure 5.7 and 5.8, examples of two participants with well predicted flexion rotations are demonstrated.
On the left side of the graph in figure 5.7, the small peak change at epoch 2 is not detected, whereas the predicted model assumes higher degrees of rotation in epoch 7. However, even though appearances of small changes is present, the predicted model follows the pattern of rotational values throughout all epochs. When looking at the corresponding bar graph, all rotational values are predicted in the correct sign.

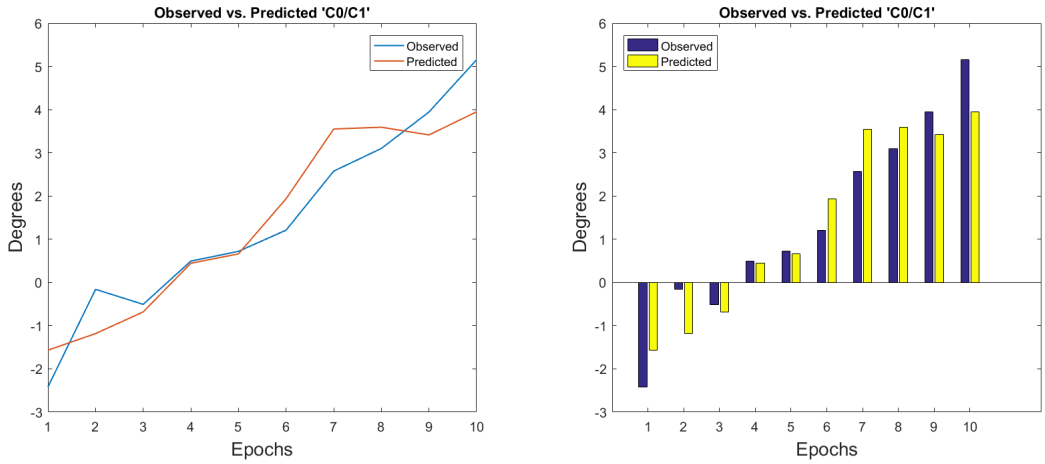

Figure 5.7: Example of well predicted joint rotation in flexion. The two figures show the full motion in "C0/C1" in participant number 29. The left side shows the plot of the data. On the right side, the bar graph from exact same movement is illustrated.

Figure 5.8 shows the observed and predicted joint "C0/C1". The rotational movement is imprecisely predicted throughout all epochs. However, it is visually apparent on both graphs, that the predicted rotation from epoch 5 to 7 is similar to the observed rotation. Since rotations are predicted in roughly the right direction as the observed data set, the overall pattern of joint movement is assumed to be retained.

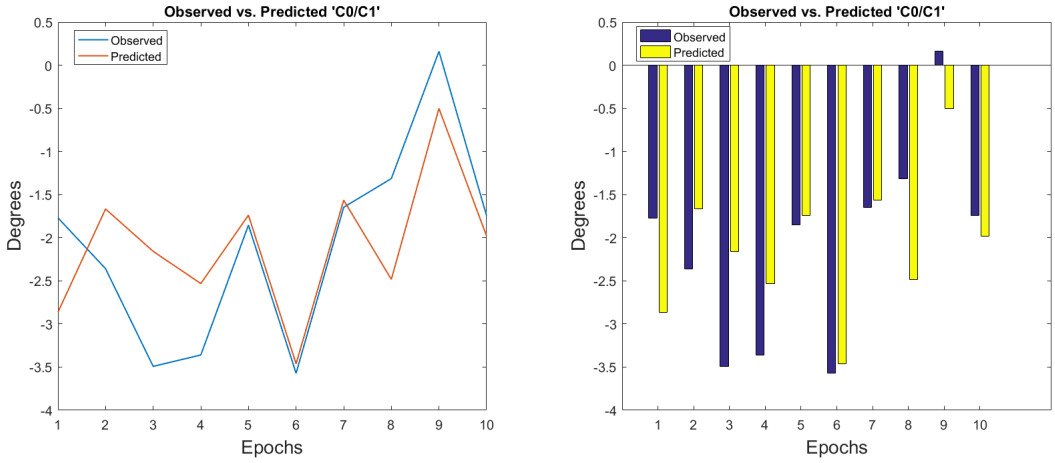

Figure 5.8: Example of a well predicted joint rotation in flexion. The two figures show the full motion in "C0/C1" in participant number 7. The left side shows the plot of the data. On the right side, the bar graph from exact same movement is illustrated.

Prediction of "C0/C1" in Extension

In the following section, results from the poorly and well predicted extension movements of joint "C0/C1" are illustrated.

Table 5.4 shows the calculated R^2 and RMSE coefficients for joint "C0/C1", when having joint "C3/C4" and "C4/C5" as predictors, hence, independent variables. The correlation between the observed and predicted rotation was calculated to be 89%, with a mean RMSE at 2.18.

	'C0/C1'
R^2	0.89 ±0.01
RMSE	2.18 ±0.04

Table 5.4: The table shows R^2 and RMSE value with mean ± std for extension.

Figure 5.9 and 5.10 show two examples of poorly predicted rotations in joint "C0/C1".

In the first figure 5.9, the predicted rotations throughout all epochs is not correlated with the observed rotations. As illustrated on the bar graph, two epochs, 1 and 7, are neither predicted in the correct sign. The error may be in the observed rotation starts from -2 in the first epoch and has a steep increase to almost 5 in the next epoch. Since a movement pattern can not be recognized, the regression does not behave sufficiently through all epochs.

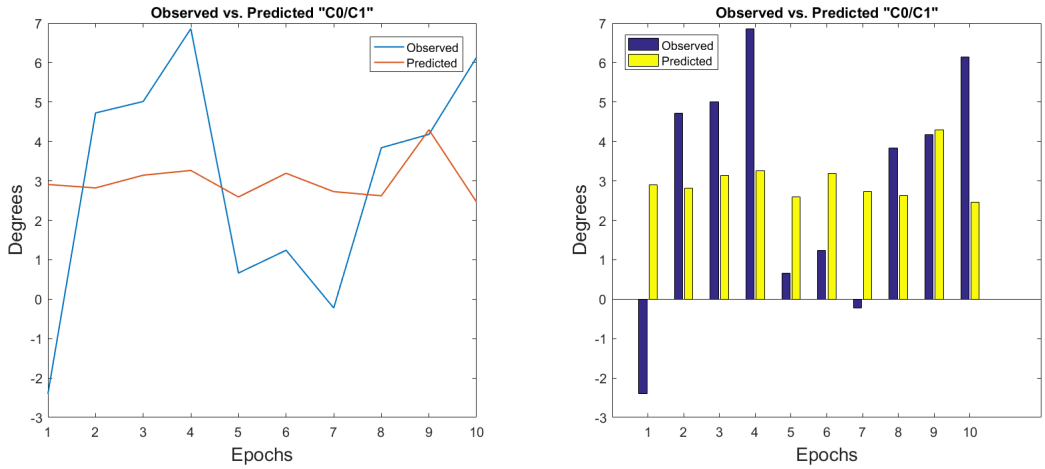

Figure 5.9: Example of weak predicted joint rotation. The two figures show the full motion in "C0/C1" in participant number 4. The left side shows the plot of the data. On the right side, the bar graph from exact same movement is illustrated.

Figure 5.10 also shows a bad prediction of the extension movement. The predicted rotation starts almost in the same degree of rotation as observed in epoch 1 and ends almost equally in epoch 10. However, it does not matter for the rest of the pattern of movement throughout all epochs, as steep changes are not taken into account. On the corresponding bar graph, a prediction in epoch 3 is also mistaken in the sign, as the predicted value is nearly -2 degrees, and the observed value is nearly +2 degrees.

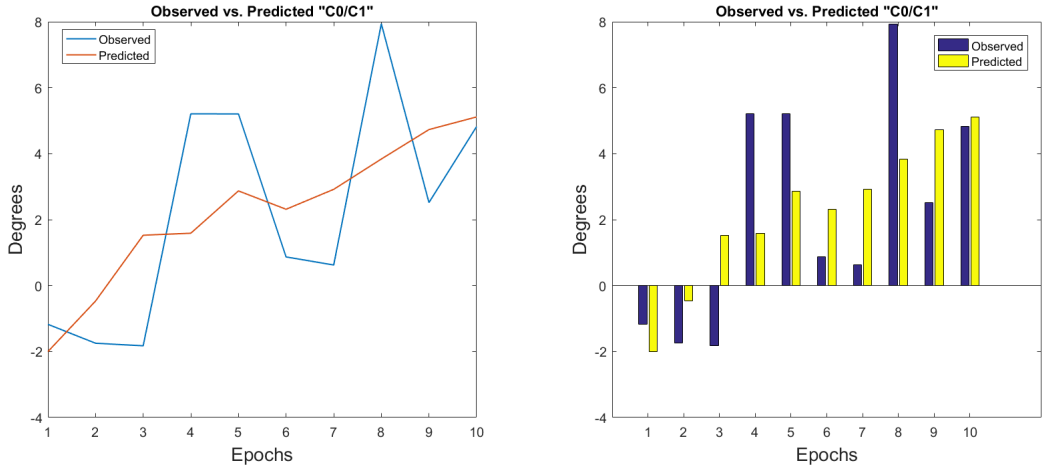

Figure 5.10: Example of weak predicted joint rotation. The two figures show the full motion in "C0/C1" in participant number 9. The left side shows the plot of the data. On the right side, the bar graph from exact same movement is illustrated.

In the following figures 5.11 and 5.12, examples of well predicted "C0/C1" joint motions are illustrated.

In figure 5.11, the predicted model follows the pattern of rotational values throughout all epochs. In epoch 3, the predicted rotation is assumed to have a slight increase, and may be due to the pattern in future movements. The upcoming peaks in epochs 5 and 8 may not be entirely accurate, but the pattern has been obtained and the movement can be described. However, even though appearances of small changes is present, the predicted rotations is assumed adequate. When looking at the corresponding bar graph, all rotational values are predicted in the correct sign.

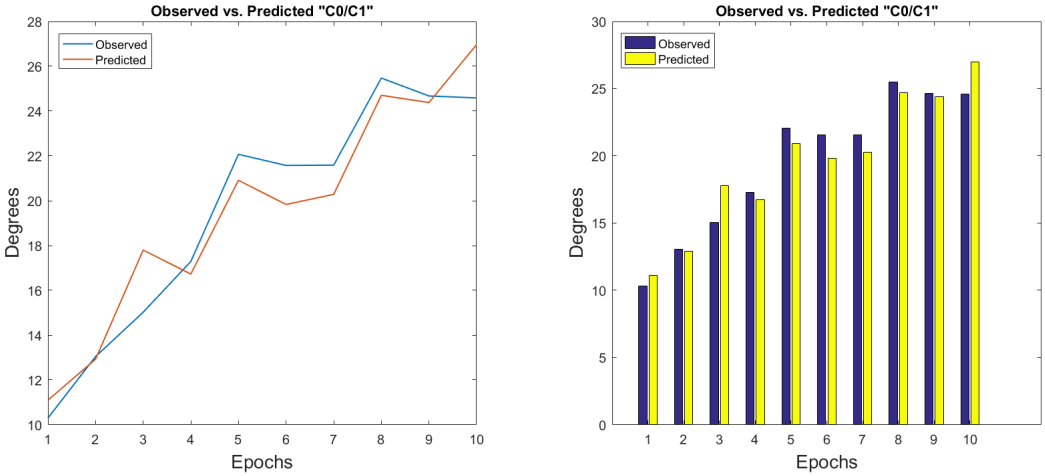

Figure 5.11: Example of strong predicted joint rotation. The two figures show the full motion in "C0/C1" in participant number 1. The left side shows the plot of the data. On the right side, the bar graph from exact same movement is illustrated.

In figure 5.12, another well predicted "C0/C1" joint movement is demonstrated. The movement through all the epochs is consistent with the observed rotations, except from in epoch

7 where the small change in degrees is not predicted. This does not affect the rest of the motion pattern as the movement almost ends in the same degree of rotation in epoch 10. On the corresponding bar graph, it is seen that the differences of the rotations are also minimal. However, all rotational values are predicted in the correct sign.

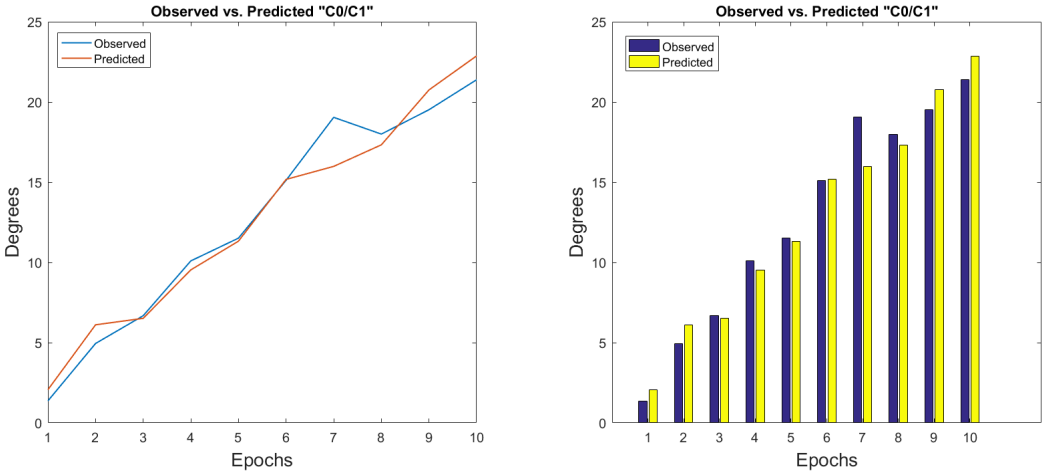

Figure 5.12: Example of strong predicted joint rotation. The two figures show the full motion in "C0/C1" in participant number 27. The left side shows the plot of the data. On the right side, the bar graph from exact same movement is illustrated.

As shown in table 5.4, the extension movements correlation is 89% in joint "C0/C1", when two predictors "C3/C4" and "C4/C5" are used.
This is lower compared to the predicted movement in table 5.2, where the correlation value is 97% when all six joints are used to predict "C0/C1". The poorer prediction is thus in line with the lower correlation value.

Division into subgroups of motion pattern

5.2 Results of division of Motion Pattern

This section answers results to Part 3.

After calculating the total ROM of each participant, k-means divided the total ROM of flexion and extension into subgroup A and B. In the observed data set, the total division of 33 participant in flexion resulted in 19 participants in group A, and 14 participants in group B (A=19, B=14). In the extension data set, with a total of 32 participants, group A consists of 17 participants and group B consists of 15 participants (A=17, B=15), see figure 5.13 for distribution.

Observed study data

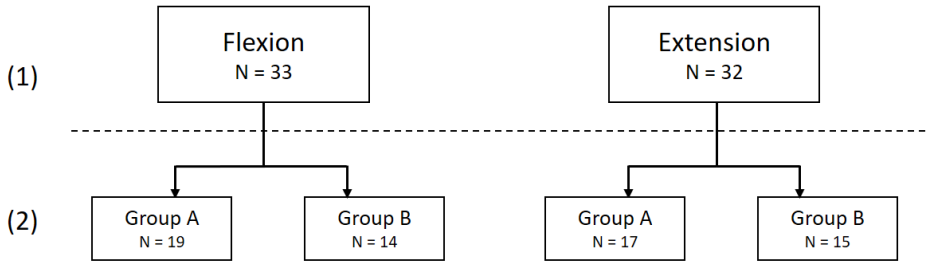

Figure 5.13: In the observed study data: (1) is the total number of participants and (2) is the new initialised subgroups after k-means partition.

Similar clustering approach was applied for the predicted data set. The k-means division of flexion resulted in 16 participants in group A, and 17 participants in group B (A=16, B=17). For the extension data set, the division resulted in 19 participants in group A and 13 participants in group B (A=19, B=13). The group division was not identical as in the observed study data, as three participants in flexion, and two participants in extension were categorised differently in the subgroups. See figure 5.14 for distribution.

Predicted data set

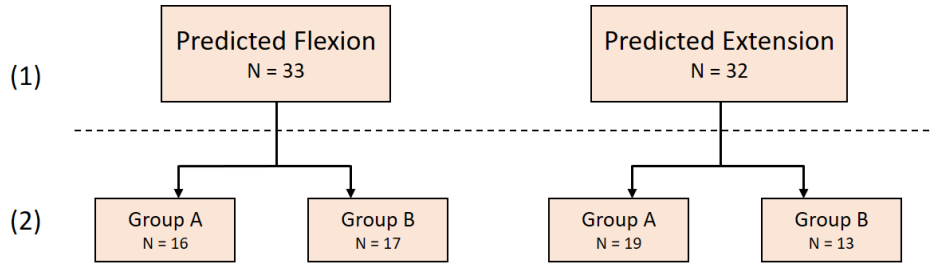

Figure 5.14: In the predicted data set: (1) is the total number of participants and (2) is the new initialised subgroups after k-means partition.

In order to make a leave one out cross validation between observed study data and predicted data set, five participants in total were excluded, i.e. three participants from the flexion movement and two from the extension movement.
The final distribution for observed study data and predicted data set is outlined in figure 5.15. The new subgroups are thus distributed, flexion: A=16, B=14 and extension: A=17, B=13.

Final distribution

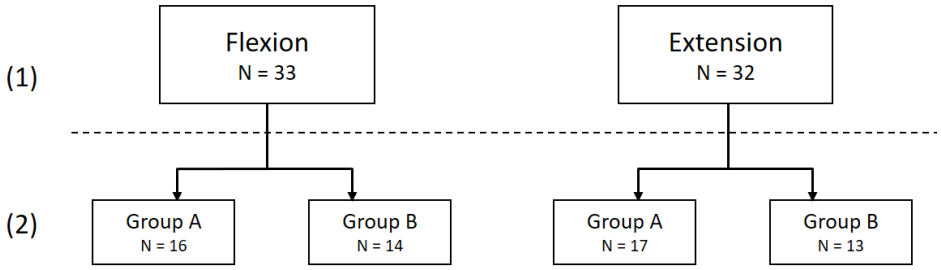

Figure 5.15: Final distribution for observed and predicted data set. (1) is the total number of participants in flexion and extension and (2) is the new initialised subgroups after excluding four participants.

5.2.1 Validation of Divided Motion Pattern

After exclusion of five participants, validation between the groups was made. Observed subgroup A and Predicted subgroup A were first trained and then tested, and Observed subgroup B and Predicted subgroup B likewise. The four subgroups regarding training and testing with LOOCV, are shown in figure 5.16. The figure 5.16, only shows flexion, thus same approach applies to the extension division.

The total ROM for flexion and extension in each subgroup are shown in the following sections.

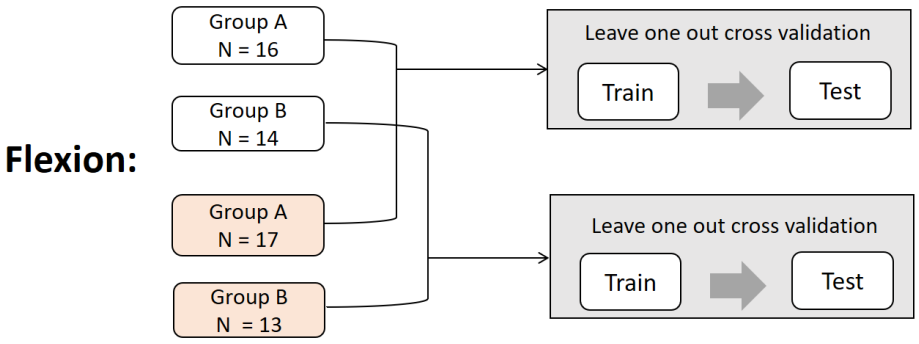

Figure 5.16: The figure shows subgroup A and subgroup B for flexion, where the white box is the observed study data, and the coloured box contains the predicted data set.

After a k-means partition, all participants' total ROM in flexion and extension were divided into subgroups. In the following tables 5.5 and 5.6, the total ROM in flexion and extension is collected. All rotational values are given in degrees. The marked red rotations shows the division of minimum and maximum rotations of each subgroup.

Observed Flexion	
Group A (N=16)	**Group B (N=14)**
-47,16	-56,985
-45,3062	-52,8148
-44,7319	-56,9362
-41,3	-60,6438
-39,8182	-63,4137
-38,2197	-58,1355
-43,2101	-71,5439
-36,6364	-56,3953
-39,2236	-62,8325
-44,4982	-57,4237
-36,0332	-53,9536
-26,277	-50,7718
-42,4416	-59,0808
-36,1148	-54,8081
-37,7759	
-44,375	

(a) Distribution of flexion groups in the observed class.

Predicted Flexion	
Group A (N=16)	**Group B (N=14)**
-46,2307	-55,9713
-42,8948	-52,0274
-44,6091	-55,6647
-40,2013	-62,7488
-39,0894	-60,4834
-31,9747	-59,2704
-42,1952	-70,6594
-35,7678	-56,9541
-39,1733	-62,6492
-40,5962	-58,0178
-35,0046	-52,7196
-26,0618	-50,1863
-41,8106	-58,9683
-36,835	-53,3369
-37,4854	
-43,7868	

(b) Distribution of flexion groups in the predicted class.

Table 5.5: (a) and (b) show the maximum rotations of each participant in flexion and the distribution in group A and B.

Observed Extension	
Group A (N=17)	**Group B (N=13)**
38,7809	60,0693
49,5914	66,2389
42,1697	81,6281
48,1841	56,5863
54,0345	58,7912
50,5858	57,1336
46,484	64,8054
54,0874	83,2833
51,2879	59,7509
47,4503	56,4418
46,3671	57,6158
52,4042	66,7102
52,6554	62,9109
45,7729	
42,0481	
40,4253	

(a) Distribution of extension groups in the observed class.

Predicted Extension	
Group A (N=17)	**Group B (N=13)**
39,0473	58,4759
51,9018	63,1189
40,5664	80,1934
47,0004	56,5988
49,1558	57,2710
47,943	54,8761
46,2194	62,527
53,7055	82,7910
47,5138	59,4839
46,2465	57,0628
47,1756	55,9662
52,1040	66,0933
52,1323	63,06699
43,6032	
40,6947	
40,2374	

(b) Distribution of extension groups in the predicted class.

Table 5.6: (a) and (b) show the maximum rotations of each participant in extension and the distribution in group A and B.

After a cross-validation with leave-one-out, the correlation values have been calculated. The table values represent how close the subgroups of observed study data were correlated with the subgroups of predicted data set.

Table 5.7 shows the calculated R^2 and RMSE values of the differences between the observed and predicted flexion rotations in group A. For instance, in the first joint "C0/C1", there is a correlation of 98% between the two groups, observed flexion A and predicted flexion A. When comparing the joints, "C2/C3" is the most eye-catching joint with the lowest correlation of 88%. This means that the maximum rotation in joint "C2/C3" of observed group A and predicted group A has varied the most.

	C0/C1	**C1/C2**	**C2/C3**	**C3/C4**	**C4/C5**	**C5/C6**	**C6/C7**
R^2	0.98 ±0.002	0.95 ±0.003	0.88 ±0.01	0.94 ±0.003	0.90 ±0.005	0.94 ±0.003	0.93 ±0.005
RMSE	0.50 ±0.02	0.83 ±0.03	0.87 ±0.03	0.72 ±0.02	0.79 ±0.02	0.90 ±0.03	1.04 ±0.03

Table 5.7: The table shows R^2 and RMSE values with mean ± std between group A for flexion movement.

Table 5.8 shows calculated R^2 and RMSE values of the difference between the observed and predicted flexion rotations in group B. Generally, the clusters of rotations in the two groups are relatively similar, as it can be seen from the high correlation values between all joints.

	C0/C1	**C1/C2**	**C2/C3**	**C3/C4**	**C4/C5**	**C5/C6**	**C6/C7**
R^2	0.98 ±0.01	0.98 ±0.004	0.93 ±0.008	0.94 ±0.003	0.97 ±0.001	0.96 ±0.003	0.93 ±0.004
RMSE	0.57 ±0.027	1.02 ±0.054	0.99 ±0.032	0.86 ±0.033	0.84 ±0.027	0.99 ±0.031	1.19 ±0.034

Table 5.8: The table shows R^2 and RMSE values with mean ± std between group B for flexion movement.

Table 5.9 shows the calculated R^2 and RMSE values of the differences between the observed and predicted extension rotations in group A. All joints showed a correlation of 94% or above, assuming that the clusters between the two groups are very similar.

	C0/C1	**C1/C2**	**C2/C3**	**C3/C4**	**C4/C5**	**C5/C6**	**C6/C7**
R^2	0.94 ±0.006	0.95 ±0.003	0.95 ±0.004	0.95 ±0.005	0.97 ±0.002	0.96 ±0.004	0.95 ±0.004
RMSE	1.17 ±0.071	0.81 ±0.024	0.81 ±0.026	0.93 ±0.058	0.76 ±0.022	0.67 ±0.018	1.67 ±0.017

Table 5.9: The table shows R^2 and RMSE values with mean ± std between group A for extension movement.

Table 5.10 shows correlation value for each joint between observed and predicted group B. The lowest and highest correlation value is 93% and 98%, respectively.

	C0/C1	**C1/C2**	**C2/C3**	**C3/C4**	**C4/C5**	**C5/C6**	**C6/C7**
R^2	0.98 ±0.002	0.93 ±0.012	0.98 ±0.003	0.94 ±0.006	0.94 ±0.005	0.97 ±0.002	0.94 ±0.008
RMSE	0.91 ±0.032	1.26 ±0.128	0.72 ±0.023	1.07 ±0.062	0.95 ±0.032	0.80 ±0.026	1.86 ±0.043

Table 5.10: The table shows R^2 and RMSE values with mean ± std between group B for extension movement.

Generally, coefficient of determination values are very high for all joints ("C0/C7"). This is due to the total ROM values of the individual participants, whose maximum rotations are very close to each other in the observed study data and the predicted data set. These rotations are illustrated in the four tables 5.5a, 5.5b, 5.6a and 5.6b, where all the participant's maximum rotations are calculated.

6 | Discussion

Intervertebral joint motion can be used to evaluate the functionality of the cervical spine to obtain a better understanding of neck pain and general back disorders. Until recently, the movement of the cervical spine was assumed as a spring model, where [Wang et al.,2017] [5] proved that in vertebral movements in the cervical spine, anti-directional movements were present. This led to disproving of the linear and continuous spring-like spine structure.
Different segmentation and tracking methods have been used to track different regions of the spinal cord, of which the cervical spine is still an area of limited research in tracking rotations of the vertebrae. Based on this thesis' research statement, segmentation methods by manually marking of each cervical vertebra corner was developed by [Nohr et al., 2017] [24], but have shown irregular tracking of the upper vertebra C1 due to change of shape during motion.
In the prediction area, the effect of muscle forces on the cervical spine has been predicted and recently published by [Abbeele et al.,2017] [30], but prediction of the cervical spine motion does not exist.

The purpose of this study was to investigate the cervical spine motion in healthy participants, by predicting every joints' (from C0 to C7) full rotation from natural upright position to end-range movement. A regression model was developed to calculate every vertebral rotation in flexion and extension direction.
This prediction model is not affected by shape changes in joints. By predicting all joint movements through regression analysis, this study can supply segmentation and tracking methods in those areas where vertebrae are irregular and difficult to track throughout video sequences.

By using multiple linear regression (MLR) for prediction, six joints were used as predictors as independent variables, to describe the full neck movement in flexion and extension. The results of the predicted 7^{th} joint motion were highly correlated with the associated observed rotational values. The coefficient of determination R^2 was used as a measure of the proportion of the variance between observed rotations against predicted rotations. For predicted flexion movement, a mean correlation for all joints could be explained by 95%, where the mean correlation could be explained by 96% in the extension movement. However, R^2 increases or stays the same as more predictors are added to the MLR model, thus R^2 alone cannot be used to help identifying predictors. Because of this, a root mean squared error (RMSE) was calculated to show model performance. The model performance was shown, by estimating the RMSE of the observed rotations against the regression line of observed vs. predicted rotations. RMSE has the same unit as the dependent variable. For the predicted flexion movement, the regression model was explained by an error of 0.55° in joint "C0/C1".

Predictions

Adding more explanatory variables into the multiple linear regression showed high correlation values, i.e 98% correlation in joint "C0/C1" for flexion, and 97% correlation in joint "C0/C1" for extension. For the lowest located cervical joint "C6/C7", the correlation value for flexion was 93%, and 95% for extension in the same joint.

The interest was about whether the dynamics could be described by fewer joints, thus two variables were chosen. The joints "C3/C4" and "C4/C5" were selected for the purpose that they are located in the middle of the cervical spine and therefore easily accessible to track during motion. The C3-C6 vertebrae are categorised as uniform in shape, thus another reason for selection of these joints. In addition, the movement of joint "C0/C1" has a greater impact on "C3/C4" and "C4/C5" during motion, than on the lower located vertebrae, for instance on "C5/C6" or "C6/C7". When using this prediction model in conjunction with vertebral tracking methods, the joints "C3/C4" and "C4/C5" are easy to track, thus "C0/C1" can be predicted.

Although the use of all joints for prediction of movements shown to have a high correlation and low error value, the results when selecting two predictors were lower in correlation and higher in error. For flexion, there was a correlation of 90% with an RMSE value of 1.25°, and for extension, the values were 89% and 2.18°, respectively. Since 40% of the movement contains anti-directional joint motions in the flexion and the extension movement, the less precise prediction by using two joints as predictors "C3/C4" and "C4/C5", can be due to anti-directional motions in the movements of the vertebrae.
Other selected joints could have had different demonstration of the dynamics, but are yet unknown. In this study, when using "C3/C4" and "C4/C5" as predictors, "C0/C1" in flexion was 90% and the "C0/C1" in extension was 89% correlated. These are not considered to be low, but since flexion and extension are two different movements in each direction which make the vertebral joints move in two different ways, distinctive predictors with the greatest importance to the movement could be examined. This means, instead of using the "C3/C4" and "C4/C5" joints for both directions, "C1/C2" and "C2/C3" joints could be used for prediction of "C0/C1" during flexion, and for instance "C4/C5" and "C5/C6" joints could be used for prediction of "C0/C1" during extension.

Another interesting question arises as whether a single joint is distinctive enough, to be able to predict the full-motion joint motion. Due to the project period, these were not carried out.

Validation

The aim of cross validation is to evaluate on the test set to make a generalised model. It is also used in order to reduce problems as overfitting, where it provides an indication of how the model will generalise on an independent data set. Cross validation is an estimate of generalisation of performance of models generated by a procedure and not of the model itself. When estimating the predictions in LOOCV, a general model is made. The patterns of the cervical joints can be so different, that by training with all but one participant, it might give high correlation values but can clinically lead to bias. Although the LOOCV deliver the best possible learner by training on n-1, the weakness of LOOCV could be the high computational cost, as it re-learns everything n-times. In validation of clustering of participants, this issue may not be present, since the number of rotations were distributed into smaller groups.

Clustering

Clustering of participants was carried out with k-means, to identify the variables that are associated with the range of motion in the cervical spine. In k-means, k was chosen to be 2, based on two requested groups A and B. k-means were able to group data sets almost equally. In the observed data set, all those falling below -47.16° were divided into flexion group A

and all scoring higher than -50.77° were divided into flexion group B. For the predicted data set, these values were -46.23° and -50.19°, respectively. The different division of participants may be due to the varying anti-directional joint motions in the observed and predicted data set.

The purpose of using k-means was to obtain uniformly divided data set by minimising the sum of point-to-centroid distance, summarized over two clusters. A manual division of the data set could be made as well, because of the bias in the form of wrong calculation, forgotten parameter, and in general very time-consuming.
The advantage of using k-means is that it is efficient run-time wise to use in large data types. The disadvantage can occur if outliers are considered as belonging to the wrong group. A last visual evaluation of the division of participants may therefore be a good idea, which might be clinically and statistically important.

Limitations

Data consisting of vertebral rotations from 33 participants was available and is a small amount of data to create a general model on. Furthermore, five participants were excluded in part 3 when dividing into subgroups of motion patterns. This choice was made on the basis of being able to validate quantitatively.
Having observed rotational values of the cervical vertebrae done by a clinician are useful, as it enables quantitative testing of the predicted product. However, it imposes some limits. In case the observed rotations are not actually perfect, by using it as a validation basis, the regression model will be developed towards a wrong end result. Hence, when a R^2 correlation value is 98%, i.e. almost completely correlated, the predicted rotation would still be off from the actual rotation.

As a part of the given study data, all included participants were healthy. This might impose restrictions, since the developed prediction model has not been tested on patients with neck disorders. Whether the developed model is applicable and will show same results in patients as in healthy participants is not known.

Perspectives

To gain more knowledge about the movement of cervical vertebrae in relation to anti-directional movements, it requires further research of its impact on the whole cervical spine rotation. This knowledge can be used to quantify the most significant cervical joint, so that the entire cervical spine's dynamics can be predicted by analysing on the most characteristic. In segmentation methods where the joint motions are challenging to track, the "two-prediction" approach can be applied.

7 | Conclusion

A predictive analysis of the healthy cervical spine movement in flexion and extension direction was made. All prediction analysis was performed using multiple linear regression, where all the participants' cervical joint flexions and extension directions were found.
With a general correlation of 93% to 98%, the developed regression model can predict the upper vertebra "C0/C1" by using six joints as predictors. The model was tested on 33 participants, with a corresponding manually calculated rotations that was regarded as ground truth.
By testing if specific characteristic joints could predict the dynamics throughout the movement, two joints "C3/C4" and "C4/C5" were selected as predictors. The result showed correlation of 90% for flexion and 89% for extension. The lower correlation can be due to anti-directional movements of joint movements. Since the movements of the cervical joint are different in individuals, some participants showed more descriptive joints for the rest of the movement than others.
Clustering of the total ROM of the observed study data and predicted data sets can be used to divide similar joint motion patterns into subgroups.

The developed regression model in this study has been varied, but generally in high correlation with the observed study data.
Based on the developed regression model, if at least two joints are known, it is possible to use the prediction model to calculate rotational movements in the cervical vertebrae.

Bibliography

[1] F. H. Martini, J. L. Nath, and E. F. Bartholomew, *Fundamentals of Anatomy & Physiology*. 9th ed., 2011.

[2] E. C. Benzel., *The Cervical Spine*. Lippincott Williand & Wilkins, a Wolters Kluwer business., 5th ed., 2012.

[3] M.-K. McCoy and H. Lampe, "Cervical instability."

[4] E. M. Flacsh, L. Eriksen, M. Koch, J. T. Ryd, E. Dibba, L. Skov-Ettrup, and K. Juel, "Sygdomsbyrden i danmark - sygdomme," 2015.

[5] X. Wang, R. Lindstroem, M. Plocharski, L. R. Østergaard, and T. Graven-Nielsen, "Cervical flexion and extension includes anti-directional cervical joint motion in healthy adults," *The Spine Journal*, 2017.

[6] W. J. Anderst, W. F. Donaldson, J. Y. Lee, and J. D. Kang, "Cervical motion segment contributions to head motion during flexion/extension, lateral bending, and axial rotation," *The Spine Journal*, 2015.

[7] A. C. Breen, D. S. Teyhen, F. E. Mellor, A. C. Breen, K. W. N. Wong, and A. Detiz, "Measurement of intervertebral motion using quantitative fluoroscopy: Report of an international forum and proposal for use in the assessment of degenerative disc disease in the lumbar spine," *Advances in Orthopedics*, 2012.

[8] R. Chowdhury, I. D. C. Wilson, C. J. Rofe, and G. Lloyd-Jones, *Radiology at a Glance*. 2010.

[9] T. Taylor, "Bones of the head and neck," 2017.

[10] O. F. Nielsen., *Anatomi og Fysiologi*. Munksgaard, 1st ed., 2012.

[11] R. D. Mootz and D. T. Hansen, *Chiropractic Technologies*. Aspen Publication, 1st ed., 1999.

[12] N. I. of Biomedical Imaging and Bioengineering, "Magnetic resonance imaging," 2017.

[13] F. E. Mellor, J. M. Muggleton, J. Bagust, W. Mason, P. W. Thomas, and A. C. Breen, "Midlumbar lateral flexion stability measured in healthy volunteers by in vivo fluoroscopy," *Spine*, vol. 34, no. 22, p. E811–E817, 2009.

[14] T. Fujimori, M. Iwasaki, Y. Nagamoto, T. Ishii, M. Kashii, T. Murase, T. Sugiura, Y. Matsuo, K. Sugamoto, and H. Yoshikawa, "Kinematics of the thoracic spine in trunk rotation - in vivo 3-dimensional analysis," *Spine*, vol. 37, no. 21, p. E1318–E1325, 2012.

[15] W. J. Anderst, E. Baillargeon, W. F. Donaldson, J. Y. Lee, and J. D. Kang, "Validation of a non-invasive technique to precisely measure in vivo three-dimensional cervical spine movement," *Spine*, vol. 36, no. 6, p. E393–E400, 2012.

[16] S.-K. Wu, L.-C. Kuo, H.-C. H. Lan, S.-W. Tsai, C.-L. Chen, and F.-C. Su, "The quantitative measurements of the intervertebral angulation and translation during cervical flexion and extension," *Eur Spine Journal*, vol. 16, pp. 1435–1444, 2007.

[17] R. C. Gonzalez and R. E. Woods, *Digital Image Processing*. 5th ed., 2008.

[18] L. Wen, D. Du, Z. Lei, S. Z. Li, and M. H. Yang, "JOTS: Joint Online Tracking and Segmentation," *Proceedings of the IEEE Computer Society Conference on Computer Vision and Pattern Recognition*, vol. 07-12-June-2015, pp. 2226–2234, 2015.

[19] I. Despotovič, B. Goossens, and W. Philips, "Mri segmentation of the human brain: Challenges, methods, and applications," *Computational and Mathematical Methods in Medicine*, vol. 2015, p. 23, 2015.

[20] H. S. K. Dongsung Kim, Hanyoung Kim, "Object-tracking segmentation method: vertebra and rib segmentation in ct images," *Proc.SPIE*, vol. 4684, pp. 4684 – 4684 – 10, 2002.

[21] A. Yilmaz, O. Javed, and M. Shah, "Object tracking: A survey," *ACM Computing Surveys*, vol. 38, p. 45.

[22] W. Frobin, P. Brinckmann, G. Leivseth, M. Biggemann, and O. Reikerås, "Precision measurement of segmental motion from flexion-extension radiographs of the lumbar spine," 1996.

[23] R. Reinartz, B. Platel, T. Boselie, H. van Mameren, H. van Santbrink, and B. ter H. Romeny, "Cervical vertebrae tracking in video-fluoroscopy using the normalized gradient field," *Med Image Comput Comput Assist Interv.*, 2009.

[24] A. K. Nøhr, L. P. Pilgaard, B. D. Hansen, R. Nedergaard, H. Haavik, R. Lindstroem, M. Plocharski, and L. R. Østergaard, "Semi-automatic method for intervertebral kinematics measurement in the cervical spine," 2017.

[25] A. Ahmadi, N. Maroufi, H. Behtash, H. Zekavat, and M. Parnianpour, "Kinematic analysis of dynamic lumbar motion in patients with lumbar segmental instability using digital videofluoroscopy," *Eur Spine Journal*, 2009.

[26] N. Bogduk and S. Mercer, "Biomechanics of the cervical spine. i: Normal kinematics," *Clinical Biomechanics*, 2000.

[27] A. Middleditch and J. Oliver, *Functional Anatomy of the Spine*. 2nd ed., 2005.

[28] J. H. Zar, *Biostatistical Analysis*. 5th ed., 2014.

[29] T. Fawcett, "An introduction to roc analysis," *Elsevier*, vol. 27, pp. 861–874, 2006.

[30] M. V. den Abbeele, F. Lia, V. Pomeroa, D. Bonneaua, B. Sandoza, S. Laportea, and W. Skallia, "A subject-specific biomechanical control model for the prediction of cervical spine muscle forces," *Clinical Biomechanics*, vol. 2017 Dec 6;51, pp. 58–66, 2017.

[31] M. A. Ritter, L. D. Harty, K. E. Davis, J. B. Meding, and M. E. Berend, "Predicting range of motion after total knee arthroplasty: clustering, log-linear regression, and regression tree analysis," *The Journal Of Bone And Joint Surgery*, vol. 85, pp. 1278–1285.

[32] A. J. Hahne, J. L. Keating, and S. C. Wilson, "Do within-session changes in pain intensity and range of motion predict between-session changes in patients with low back pain?," *Australian Journal of Physiotherapy*, vol. 50, pp. 17–23.

[33] R. O. Duda, P. E. Hart, and D. G. Stork, *Pattern Classification (2nd Ed)*. Wiley, 2nd ed., 2001.

[34] R. Polikar, "Pattern recognition," *Wiley Encyclopedia of Biomedical Engineering*, 2006.